CENTRE NATIONAL DE LA RECHERCHE SCIENTIFIQUE

s m
d d e

Nancy-Université
Université Henri Poincaré
ESSTIN
UNIVERSITÉ HENRI POINCARÉ - NANCY 1

50 Years After
The Mössbauer Effect Today and in the Future
9-10 0ctober 2008- München (Bayern)

Green Rusts and Fougerite;
From Mineralogy and Environmental Science to Corrosion

Jean-Marie R. Génin

Institut Jean Barriol
Service Matériaux pour le Développement Durable et l'Environnement
UMR 7036 CNRS-Université Henri Poincaré-Nancy 1,
Département Matériaux et Structures, ESSTIN,
1 rue Jean Lamour, F-54500 Vandoeuvre-lès-Nancy,
France.
genin@esstin.uhp-nancy.fr

Why go to Mars when there are so many things to understand under our feet on Earth?

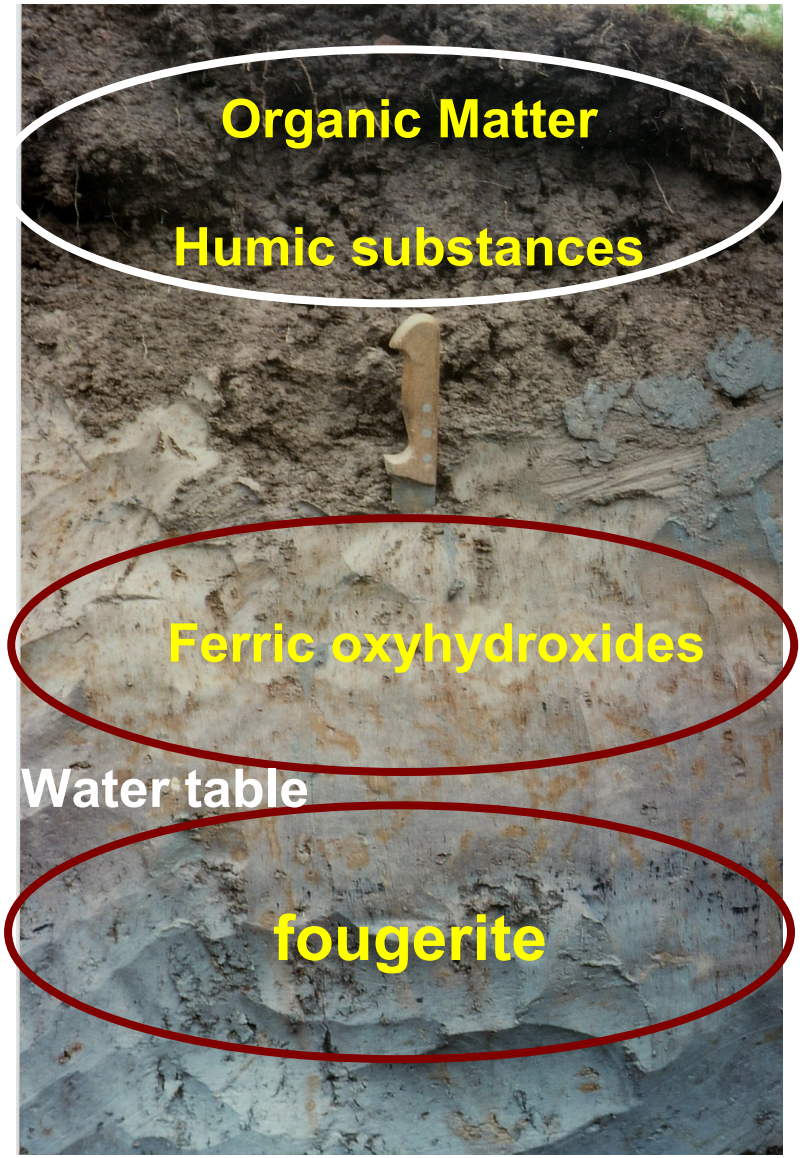

Hydromorphic soil
Gleysol

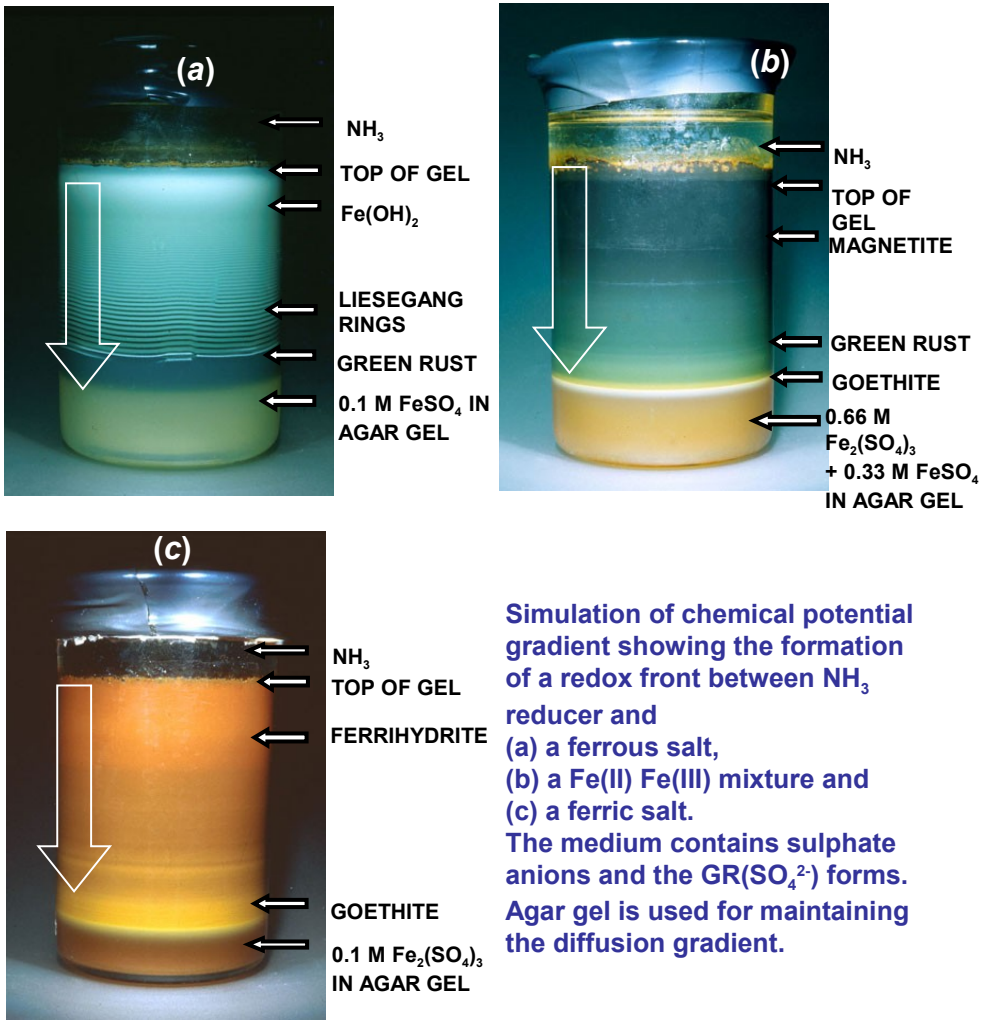

Simulation of chemical potential gradient showing the formation of a redox front between NH_3 reducer and
(a) a ferrous salt,
(b) a Fe(II) Fe(III) mixture and
(c) a ferric salt.
The medium contains sulphate anions and the GR(SO_4^{2-}) forms.
Agar gel is used for maintaining the diffusion gradient.

About ¼ of the annual production of iron is destroyed every year by corrosion.

Secret of passivation!

Corrosion is the dissolution of a metal due to its oxidation.

In the case of iron, the sequence is: $Fe^0 \rightarrow Fe^{2+} \rightarrow Fe^{3+}$

Oxidation of iron is

$$Fe^0 \Rightarrow Fe^{2+} + 2\ e^-$$

$$Fe^{2+} \Rightarrow Fe^{3+} + e^-$$

This is due to the reduction of oxidants, e. g.

$$O_2 + 4\ H^+ + 4\ e^- \Rightarrow 2\ H_2O$$

$$2\ H^+ + 2\ e^- \Rightarrow H_2$$

Fe^{2+}_{aq} exists in a wide range of pH, whereas Fe^{3+}_{aq} necessitates an acidic solution (pH < 4)

To predict corrosion, one draws the electrode potential E_h versus pH graph

We shall complete the E_h-pH Pourbaix diagrams by introducing the intermediate Fe^{II-III} compounds, the green rusts

Layered double hydroxides

Green rusts

$[Fe^{II}_{(1-x)}\ Fe^{III}_{x}\ (OH)_2\ ]^{x+}$ $[(x/n)A^{n-}\bullet(mx/n)H_2O]^{x-}$

Layer Interlayer

Anions

Cl^-, CO_3^{2-}, SO_4^{2-}, $HCOO^-$, $C_2O_4^{2-}$, SeO_4^{2-} …

Chloride	$[Fe^{II}_2\ Fe^{III}\ (OH)_6]^+ \bullet [\ Cl^- \bullet 2\ H_2O]^-$
Sulphate	$[Fe^{II}_4\ Fe^{III}_2\ (OH)_{12}]^{2+} \bullet [\ SO_4^{2-} \bullet 8\ H_2O]^{2-}$
Carbonate	$[Fe^{II}_4\ Fe^{III}_2\ (OH)_{12}]^{2+} \bullet [\ CO_3^{2-} \bullet 3\ H_2O]^{2-}$

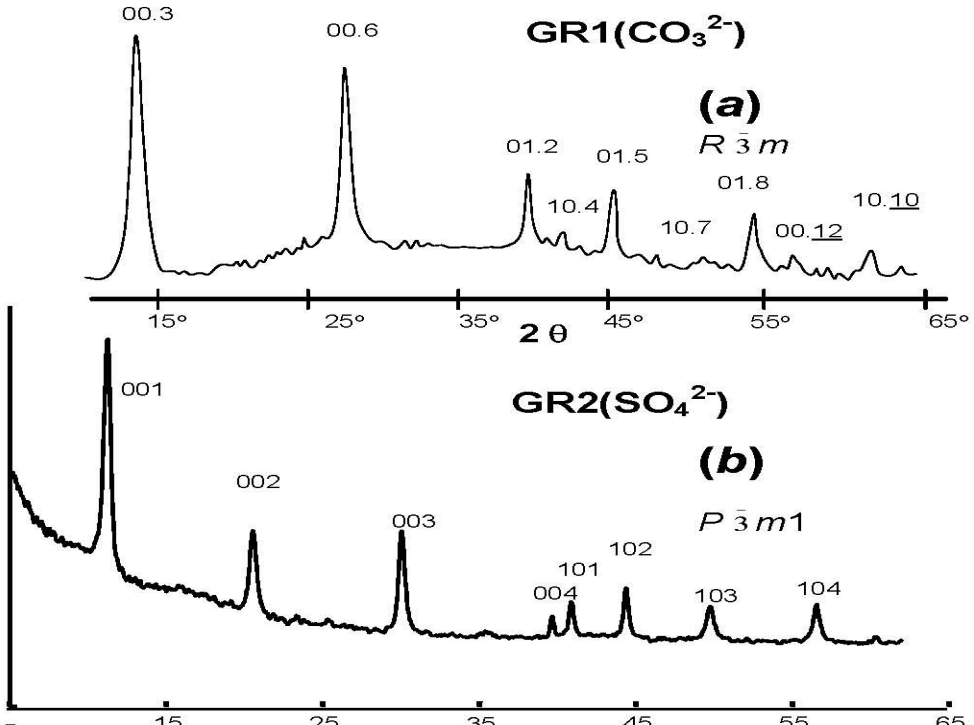

Two types of stacking

XRD pattern of hydroxycarbonate $GR1(CO_3^{2-})$.

(thesis of Omar Benali 2002).

R-3m

XRD pattern of hydroxysulphate $GR2(SO_4^{2-})$

(thesis of Rabha Aïssa 2004).

P-3m1

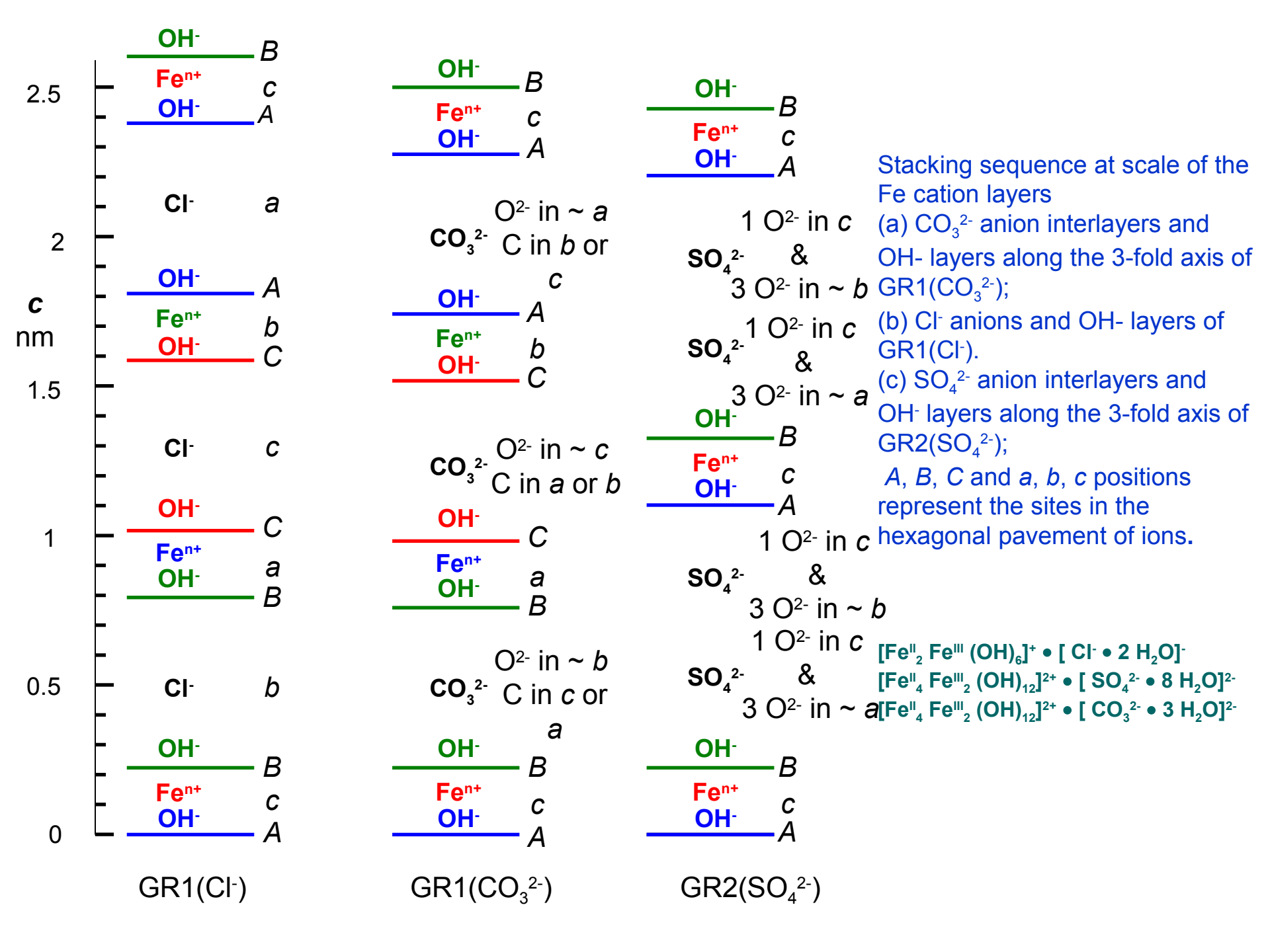
c nm
2.5
2
1.5
1
0.5
0
OH- B
Fen+ c
OH- A
Cl- a
OH- A
Fen+ b
OH- C
Cl- c
OH- C
Fen+ a
OH- B
Cl- b
OH- B
Fen+ c
OH- A
GR1(Cl-)
OH- B
Fen+ c
OH- A
O2- in ~ a
CO32- C in b or c
OH- A
Fen+ b
OH- C
O2- in ~ c
CO32- C in a or b
OH- C
Fen+ a
OH- B
O2- in ~ b
CO32- C in c or a
OH- B
Fen+ c
OH- A
GR1(CO32-)
OH- B
Fen+ c
OH- A
1 O2- in c
SO42- &
3 O2- in ~ b
1 O2- in c
SO42- &
3 O2- in ~ a
OH- B
Fen+ c
OH- A
1 O2- in c
SO42- &
3 O2- in ~ b
1 O2- in c
SO42- &
3 O2- in ~ a
OH- B
Fen+ c
OH- A
GR2(SO42-)
Stacking sequence at scale of the Fe cation layers
(a) CO3 2- anion interlayers and OH- layers along the 3-fold axis of GR1(CO3 2-);
(b) Cl- anions and OH- layers of GR1(Cl-).
(c) SO4 2- anion interlayers and OH- layers along the 3-fold axis of GR2(SO4 2-);
A, B, C and a, b, c positions represent the sites in the hexagonal pavement of ions.
[Fe II 2 Fe III (OH)6]+ • [Cl- • 2 H2O]-
[Fe II 4 Fe III 2 (OH)12]2+ • [SO4 2- • 8 H2O]2-
[Fe II 4 Fe III 2 (OH)12]2+ • [CO3 2- • 3 H2O]2-

Transmission Mössbauer spectra measured at 78 K of various Green Rusts

2 ferrous doublets D_1 & D_2 (large Δ)

1 ferric doublet D_3 (small Δ)

$x = Fe^{III} / Fe_{total}$ is obtained directly from the spectrum (RA of D_3)

Experimentally

$0.25 < x < 0.33$

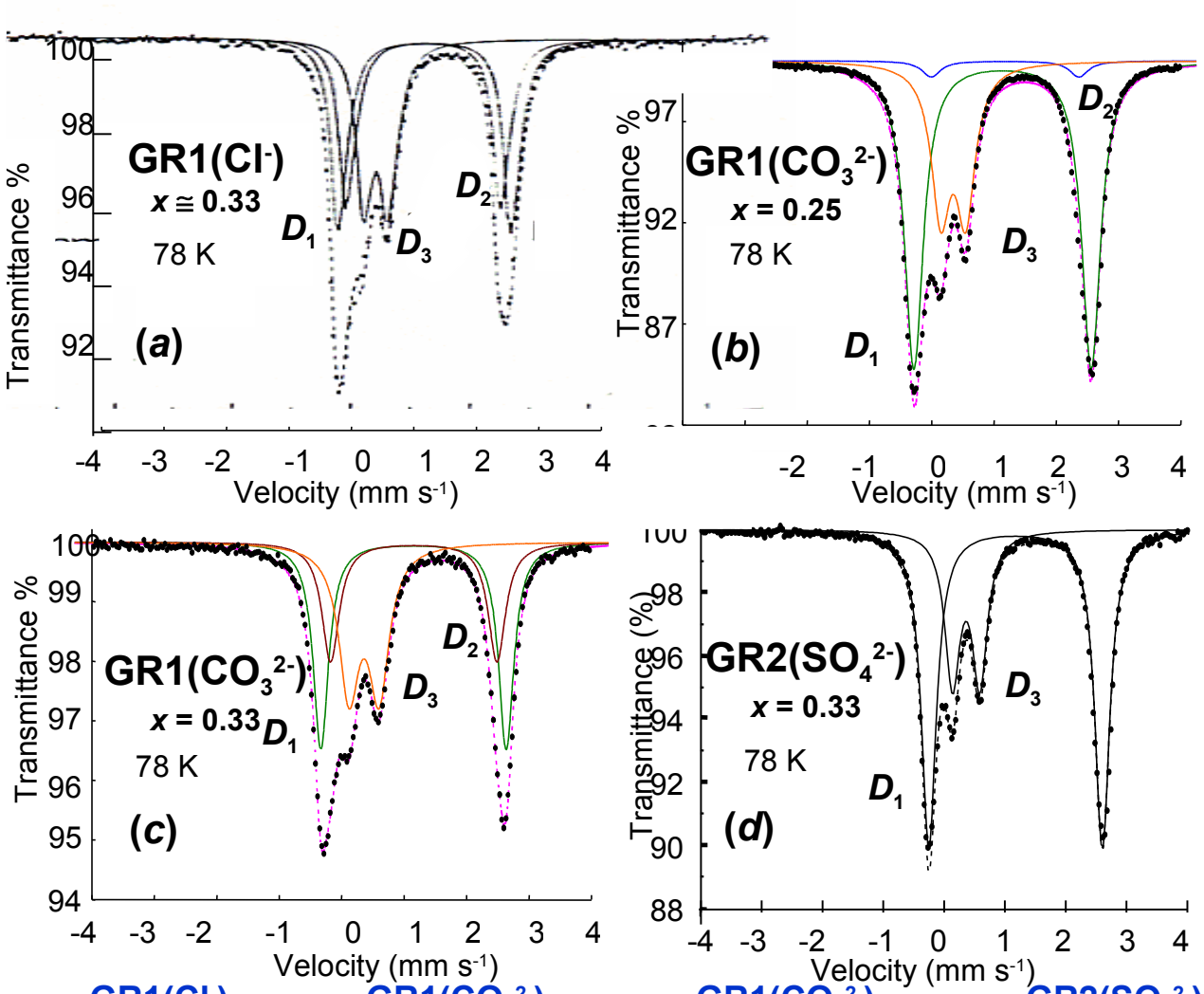

	GR1(Cl⁻)			GR1(CO_3^{2-})			GR1(CO_3^{2-})			GR2(SO_4^{2-})		
x	0.33			0.25			0.33			0.33		
	δ	Δ	RA	δ	Δ	RA	δ	Δ	RA	δ	Δ	RA
	mm s⁻¹		%	mm s⁻¹		%	mm s⁻¹		%	mm s⁻¹		%
D_1	1.27	2.89	37	1.28	2.97	62	1.27	2.93	51	1.27	2.88	66
D_2	1.25	2.60	32	1.28	2.55	12	1.28	2.64	15			
D_3	0.47	0.41	31	0.47	0.43	26	0.47	0.42	34	0.47	0.44	34

The **Fe^{II-III} hydroxycarbonate** can be prepared by **coprecipitation** of a mixture of ferrous and ferric salts in the presence of carbonate ions when adding NaOH solution. Mössbauer spectra measured at 78 K demonstrate that the range of composition for $x = [Fe^{III}]/[Fe_{total}]$ is limited to [1/4, 1/3] since for x > 1/3 there exists two phases , the Green rust at x = 1/3, $GR(CO_3^{2-})$, and another phase, α-FeOOH.

The spectrum of $GR(CO_3^{2-})$ consists of 2 ferrous doublets D_1 and D_2 with large quadrupole splitting Δ and one ferric doublet D_3 with small splitting.

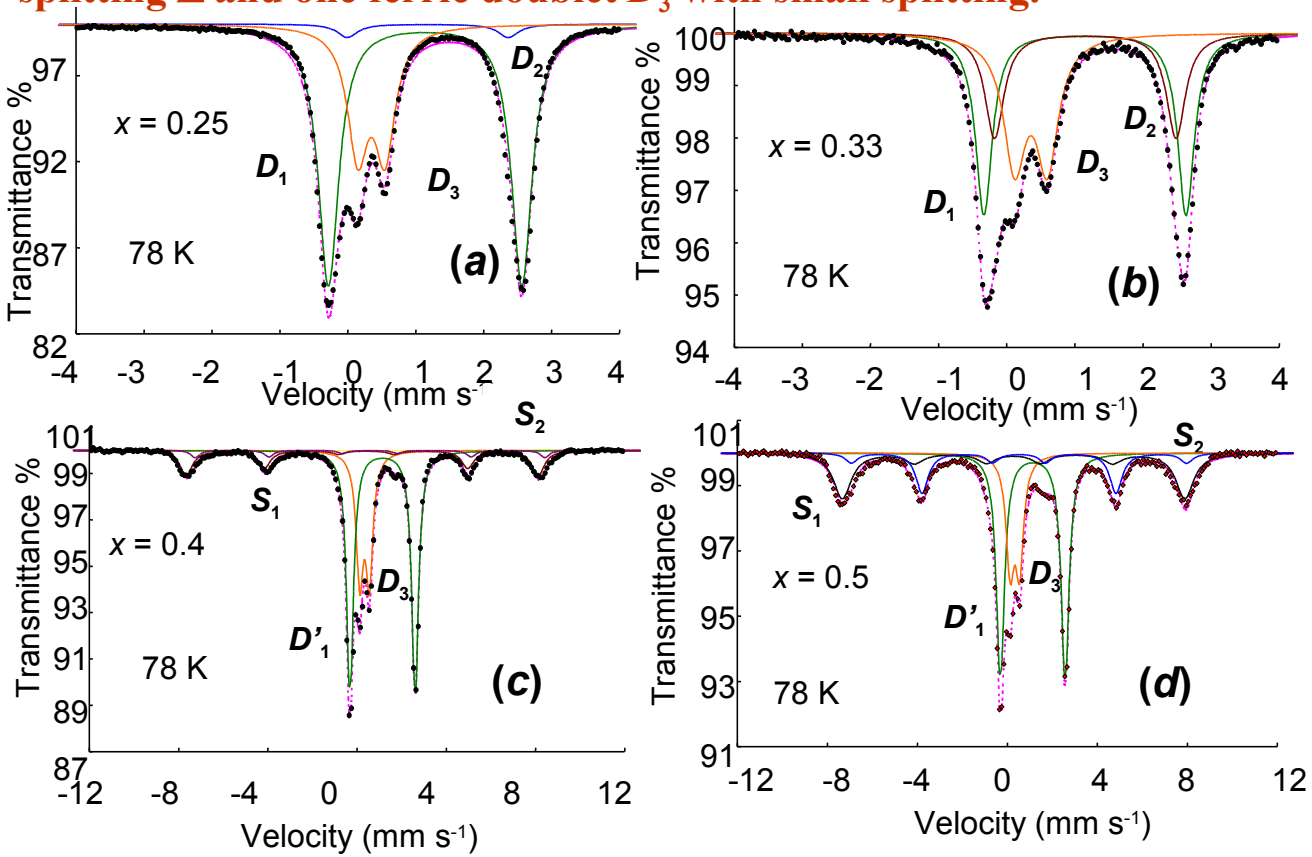

x = 0.25	D_1	D_2	D_3
δ	1.28	1.28	0.47
Δ	2.97	2.55	0.43
RA	62	12	26

x = 0.33	D_1	D_2	D_3
δ	1.28	1.28	0.47
Δ	2.97	2.55	0.43
RA	48	18	34

x = 0.4	D_1+D_2	D_3	S_1	S_2
H			490	482
δ	1.30	0.50	0.43	0.54
Δ	2.9	0.47	0	0
RA	52	25	17	6

x = 0.5	D_1+D_2	D_3	S_1	S_2
H			473	453
δ	1.29	0.49	0.39	0.53
Δ	2.87	0.48	0	0
RA	39	19	26	16

Hyperfine parameters
H (kOe), δ and Δ (mm s^{-1}), RA(%)

Fe^{II}-Fe^{III} ions coprecipitation giving for x > 1/3 a mixture of phases: $GR(CO_3^{2-})$ and goethite

$Fe^{II}_{(1-y)}Fe^{III}_y(OH)_2$ (y/2)CO_3 with 1/4< y < 1/3

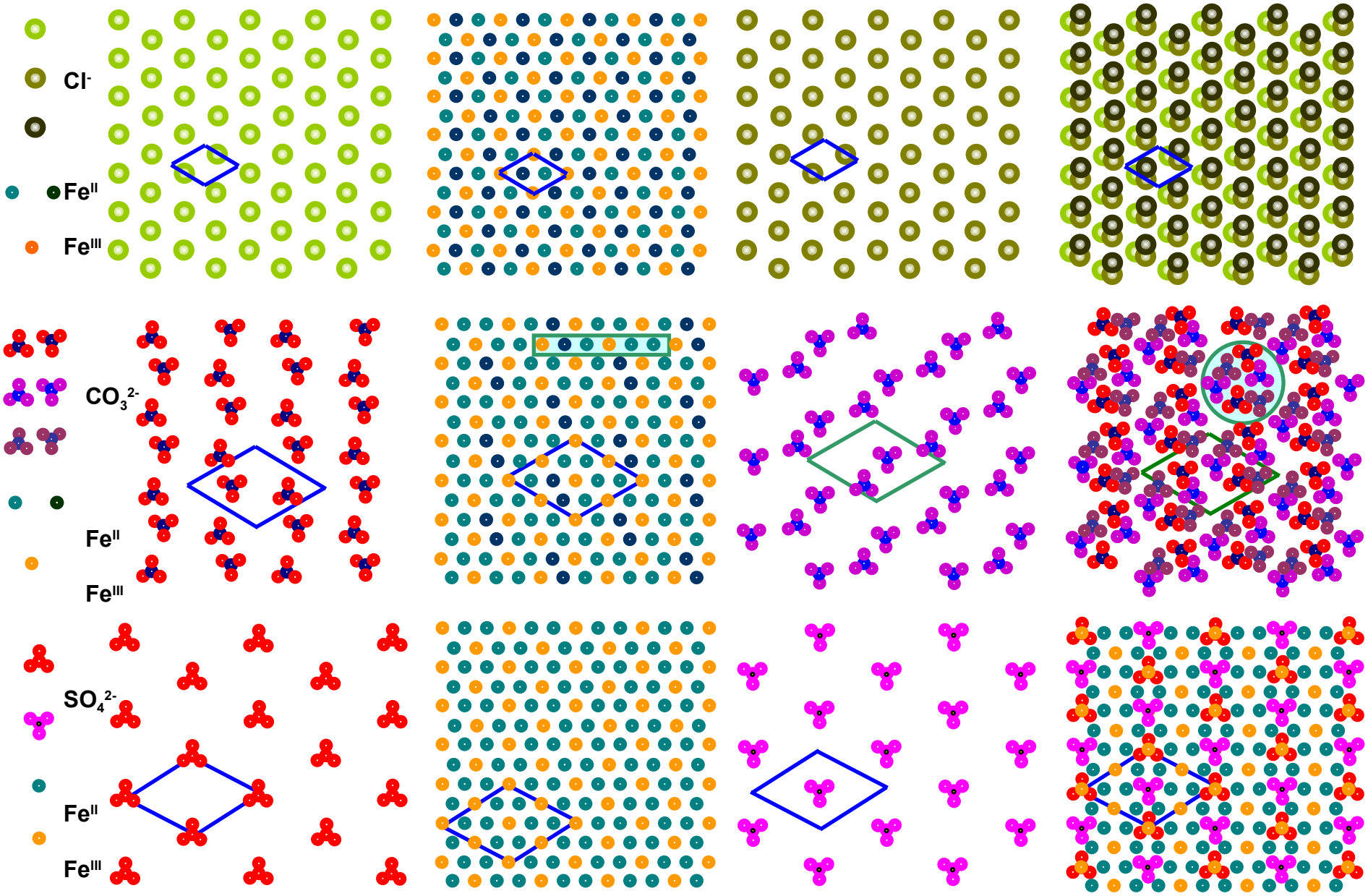

Projections perpendicular to the *c* axis of the GR structure of, from left to right, GR1(Cl^-), GR1(CO_3^{2-}) and GR2(SO_4^{2-}). OH^- ion layers are not taken into account; (a) one anion interlayer, (b) a Fe layer and (c) the next interlayer; (d) superimposition of (a), (b), (c) where only one Fe layer in the way between two interlayers is represented; (e) three adjacent interlayers in GR1s.

With synchrotron

$GR(CO_3^{2-})$ *R(-3)m* *a* = 0.317588(2) nm *c* = 2.27123(3) nm

R. Aissa, M. Francois, C. Ruby, F. Fauth, G. Medjahdi, M. Abdelmoula, J.-M. Génin
Formation and crystallographical structure of hydroxysulphate and hydroxycarbonate green rusts synthetised by coprecipitation • *J. Phys. Chem. Solids, 67* (2006) 1016-1019.

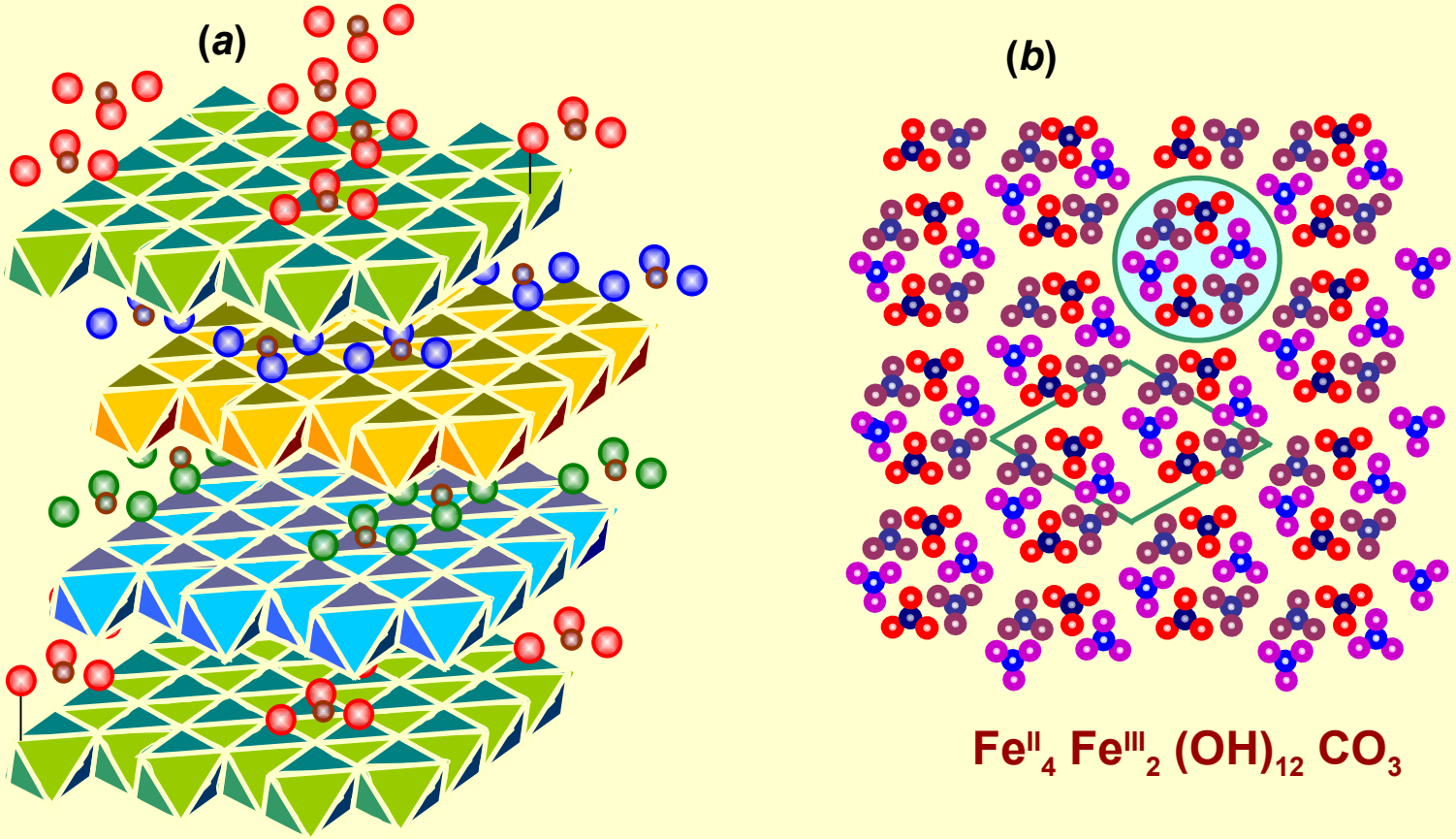

Structure of $GR(CO_3^{2-})$ Fe^{II-III} hydroxycarbonate at *x* = (1/3); (a) Three-dimensional view of the stacking of brucite-like layers. OH^- ions lie at the apices of the octahedrons surrounding the Fe cations. CO_3^{2-} ions in interlayers.
(b) Projections along the *c* axis of the CO_3^{2-} anions for three interlayers constituting a repeat.

Génin, J.-M. R.; Aissa, R.; Géhin, A.; Abdelmoula, M.; Benali, O.; Ernstsen, V.; Ona-Nguema, G.; Upadhyay, C.; Ruby, C. Fougerite and Fe^{II-III} hydroxicarbonate green rust; ordering, deprotonation and/or cation substitution; structure of hydrotalcite-like compounds and mythic ferrosic hydroxide $Fe(OH)_{(2+x)}$. *Solid State Sci.*, *7* (2005) 545-572.

The *usual* oxidation of green rusts by dissolution and precipitation

- Most of the time the corrosion of iron ends into a ferric oxyhydroxide that is the result of the oxidation of the green rust by dissolution and precipitation

Chloride containing medium

End products of oxidation
The common rusts

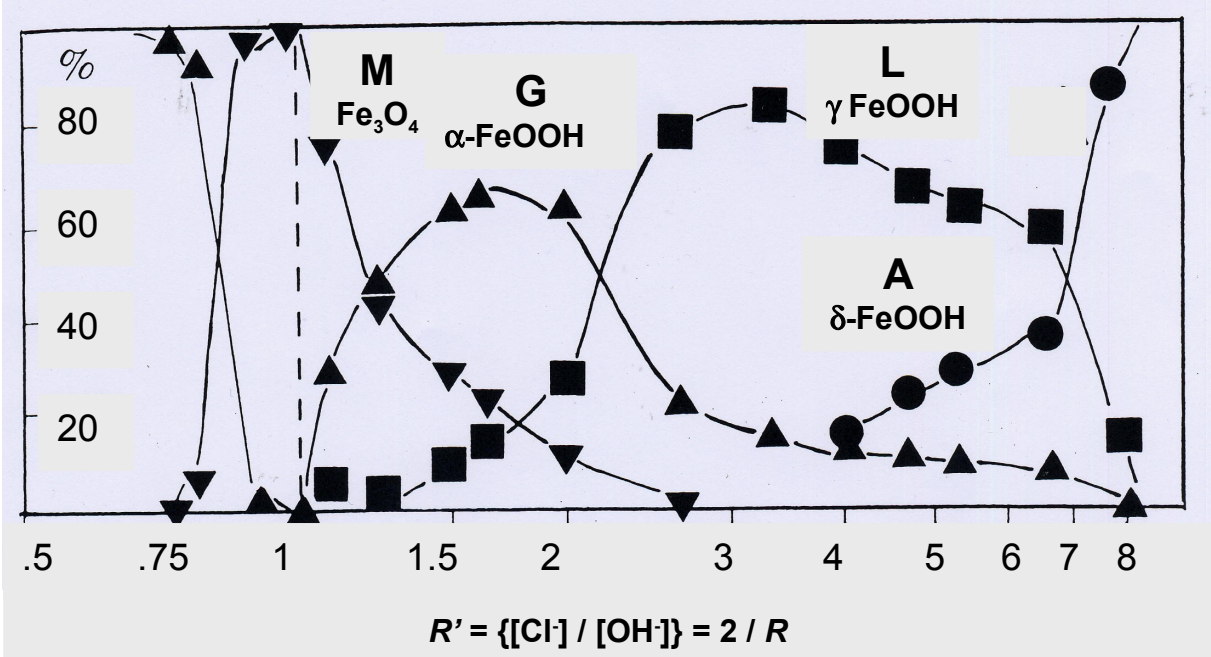

End products of the aerial oxidation of $Fe(OH)_2$, in the chloride containing medium with respect to the initial ratio *R'* = {[Cl^-] / [OH^-]} = 2 / *R*.

$R = [Fe^{III}][Fe_{total}]$ **D. Rézel 1986**

▼ **M : magnetite,** ▲ **G : goethite,** ■ **L : lepidocrocite ,** ● **A : akaganeite**

Sulphate containing medium

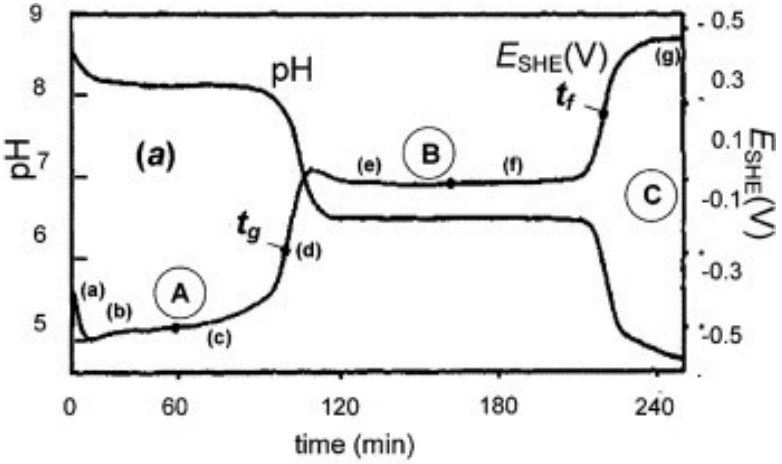

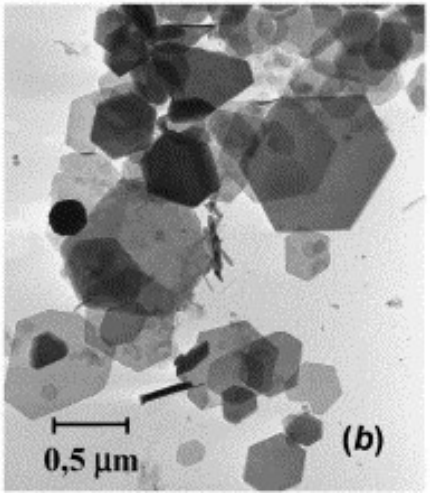

A. Olowe
Ph. Refait

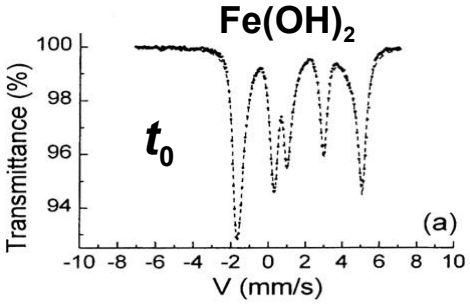

Mössbauer spectra measured at 15 K

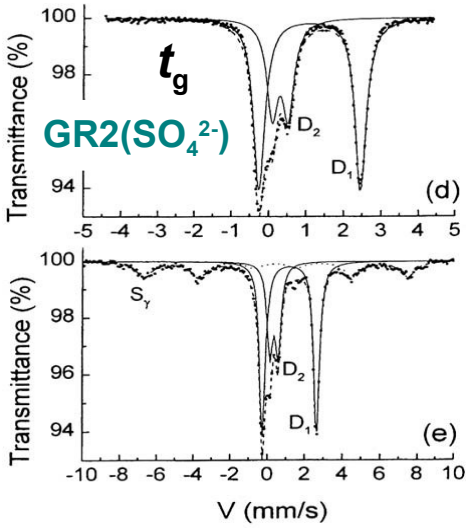

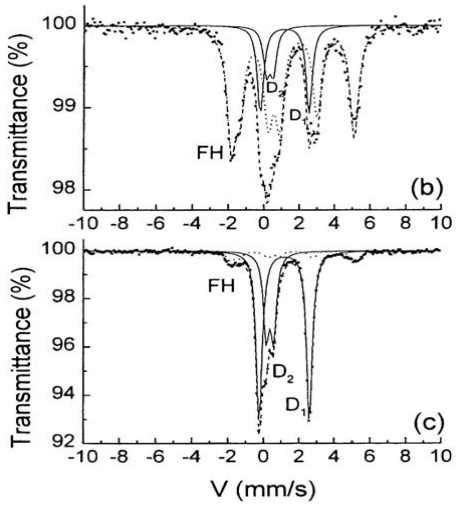

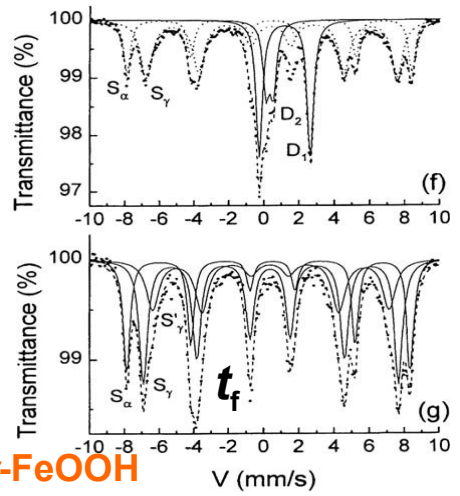

γ-FeOOH

(a) Zero-current potential E_h (SHE) and pH vs. time curves recorded during the oxidation of an aerated suspension of ferrous hydroxide in a sulphate containing medium for initial ratio $R = \{[OH^-]/[Fe_{total}]\} = R_g = 1.67$. Three stages *A*, *B* and *C* illustrated by plateaus when E_h and pH stay constant correspond to three equilibrium reactions. At t_g, 100% of GR2(SO_4^{2-}) forms and at t_f there exist only one solid phase, lepidocrocite γ-FeOOH with Fe^{II} ions within solution. Points (a)–(g) indicate the times at which the precipitates analysed by Mössbauer spectroscopy were sampled [6].
(b) Transmission electron micrograph of sample of GR2(SO_4^{2-}) at t_g [6].

Mass balance diagram comprising stoichiometric Fe^{II-III} hydroxysulphate green rust $GR2(SO_4^{2-})$ at x = 1/3. The path followed during the aerial oxidation of $Fe(OH)_2$ with an excess of Fe^{2+}_{aq} is stressed displaying the 3 stages, AB, BC, CD, as observed in E_h or pH *versus* time curves (inset). The final ferric oxyhydroxide is lepidocrocite at point C (stage 2) that transforms slowly into goethite (stage 3) from C to D in acidic conditions providing some Fe^{III} ions into solution..

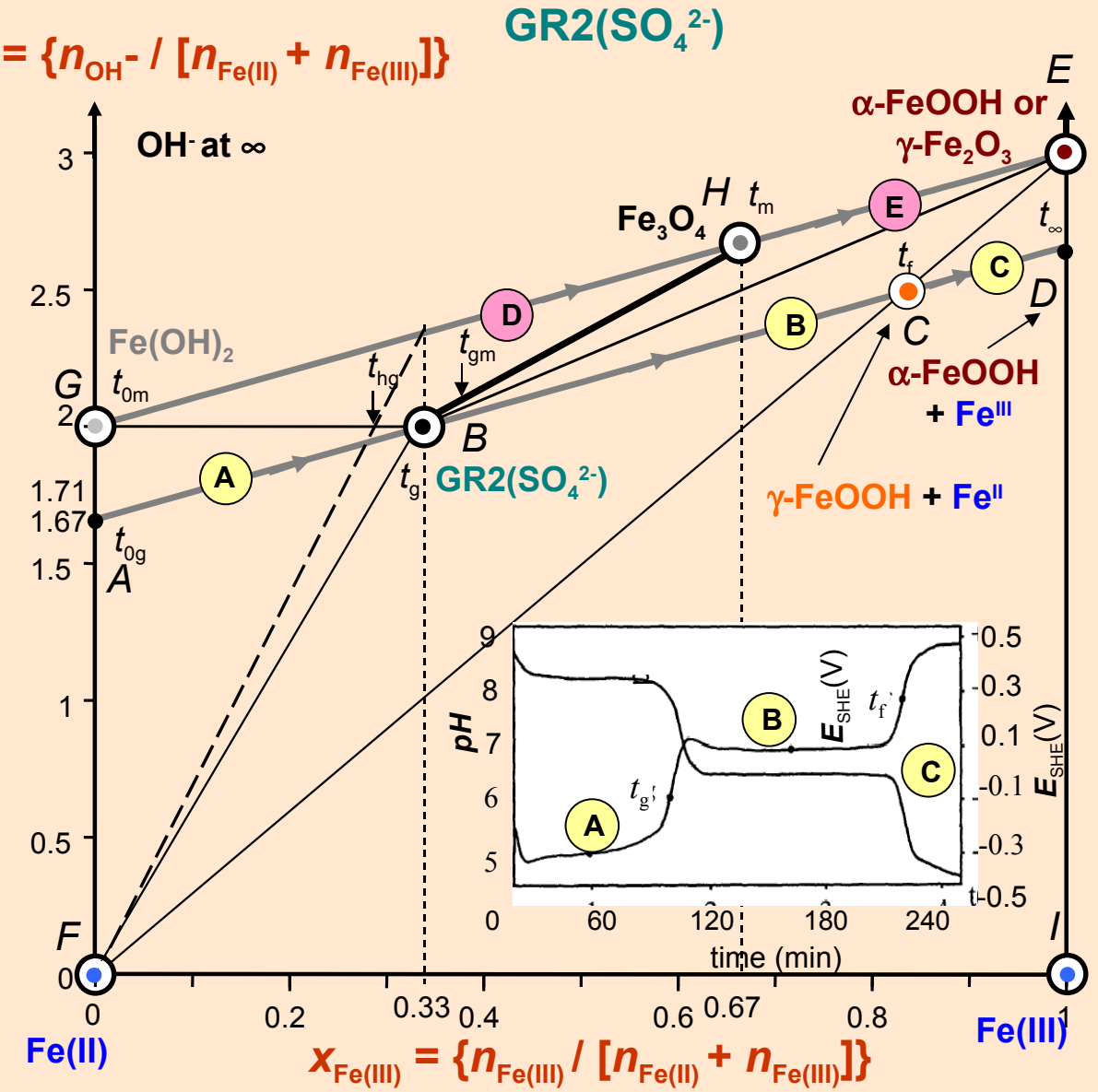

Mass balance diagram of iron compounds

A. Géhin 2004

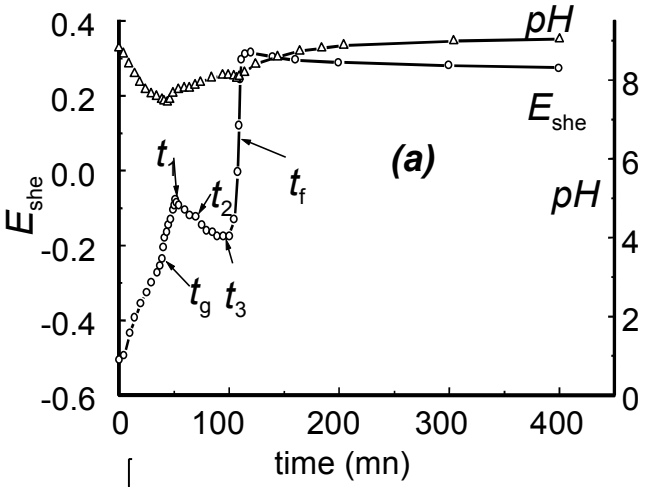

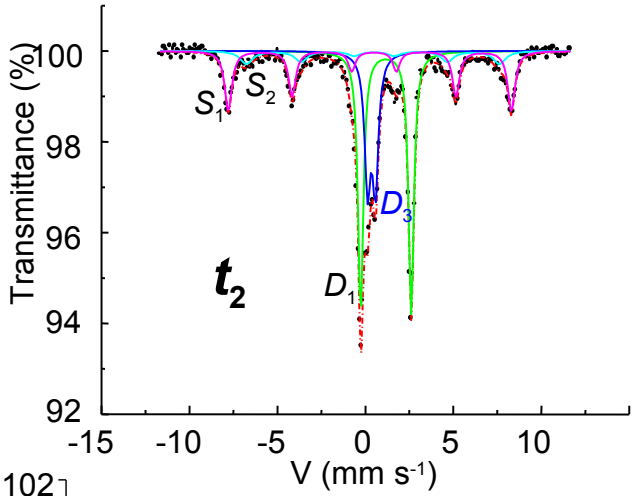

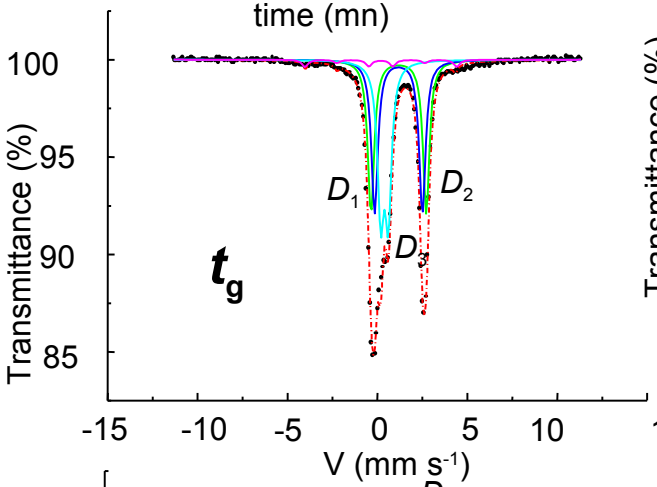

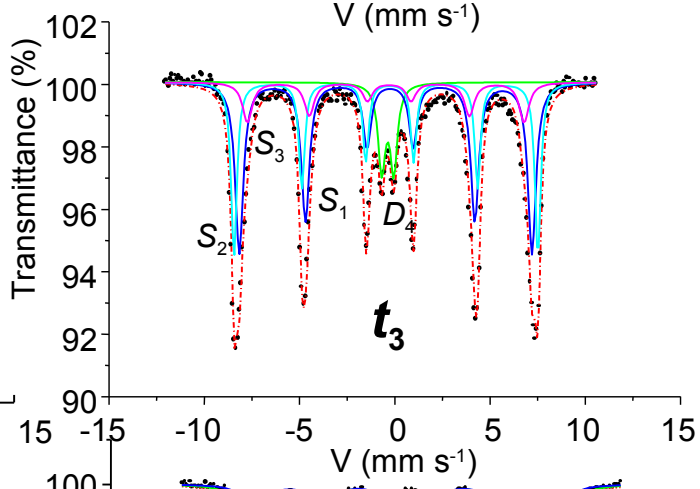

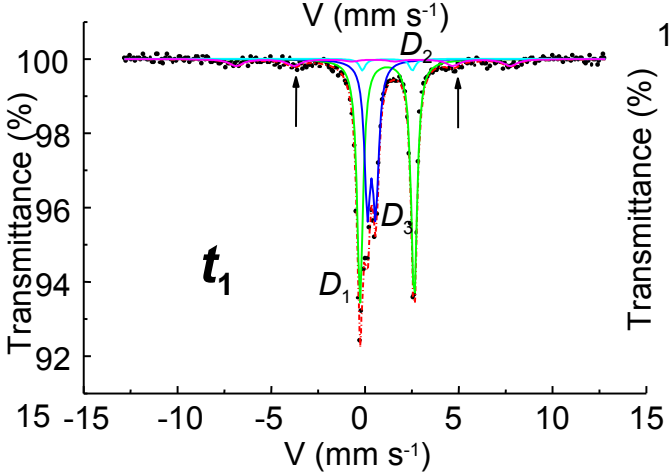

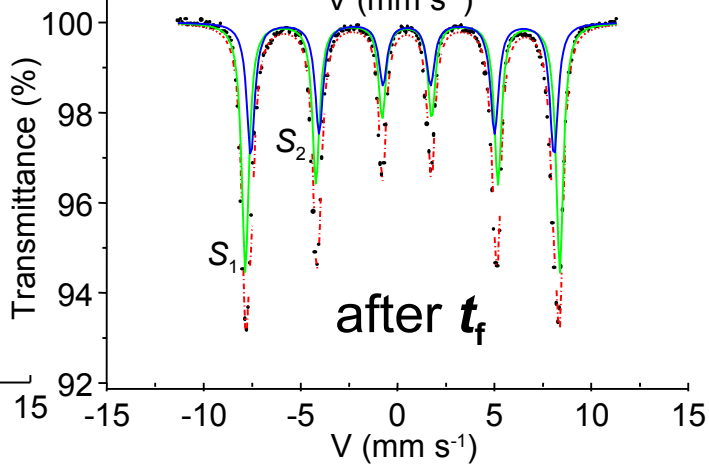

Carbonate containing medium

D_1, D_2, D_3 : GR1(CO_3^{2-}) doublets
S_1 : ferrihydrite sextet
S_2, S_3 : goethite sextets
D_4 : ferrihydrite doublet

t_g : GR1(CO_3^{2-}) alone

t_1 : GR1(CO_3^{2-}) + some ferrihydrite

t_2 : GR1(CO_3^{2-}) + goethite + ferrihydrite

t_3 : goethite + ferrihydrite

After t_f : goethite alone

O. Benali

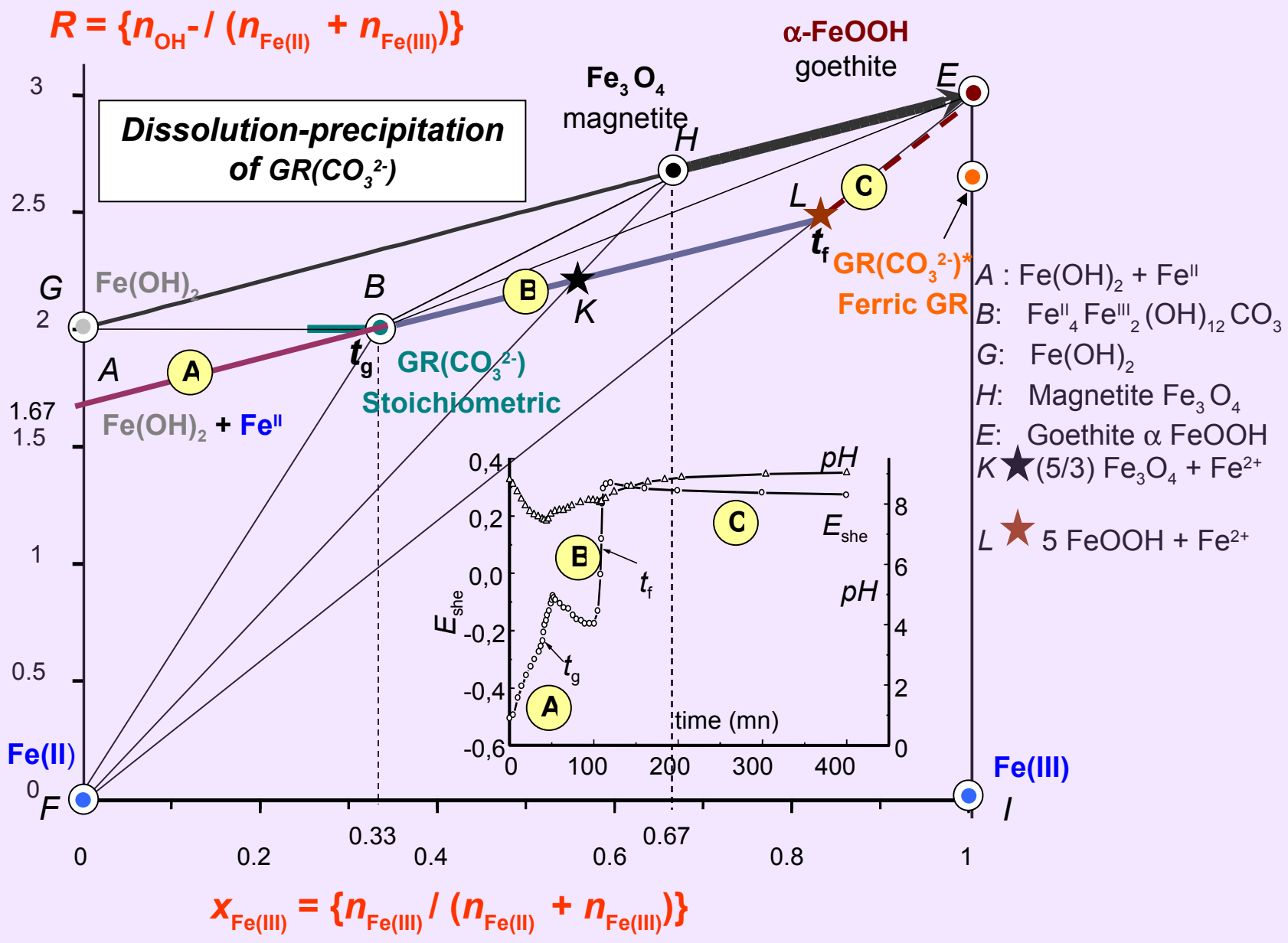

Mass balance diagram of iron compounds

Oxidation of GR2(SO_4^{2-}) and GR1(CO_3^{2-}) Lepidocrocite *versus* ferrihydrite & goethite

Stage A

$$5\ Fe^{II}(OH)_2 + SO_4^{2-} + Fe^{2+}_{aq} + (1/2)O_2 + H_2O \Leftrightarrow Fe^{II}_4Fe^{III}_2(OH)_{12}SO_4$$

$$5\ Fe^{II}(OH)_2 + CO_3^{2-} + Fe^{2+}_{aq} + (1/2)\ O_2 + H_2O \Leftrightarrow Fe^{II}_4Fe^{III}_2(OH)_{12}CO_3$$

Stage B

$$Fe^{II}_4Fe^{III}_2(OH)_{12}SO_4 + (3/4)O_2 \Leftrightarrow 5\ \gamma\text{-}Fe^{III}OOH + SO_4^{2-} + Fe^{2+}_{aq} + (7/2)H_2O$$

$$Fe^{II}_4Fe^{III}_2(OH)_{12}CO_3 + (3/4)O_2 \Leftrightarrow 5\ Fe^{III}OOH + CO_3^{2-} + Fe^{2+}_{aq} + (7/2)H_2O$$

Stage C

$$3\ Fe^{2+}_{aq} + (1/4)O_2 + (3/2)\ H_2O \Leftrightarrow \alpha\text{-}Fe^{III}OOH + 2\ Fe^{3+} + H_2$$

$$Fe^{2+}_{aq} + (1/4)O_2 + 2\ OH^- \Leftrightarrow \alpha\text{-}Fe^{III}\ OOH + (1/2)H_2O$$

As a whole

$$5\ Fe^{II}(OH)_2 + Fe^{2+}_{aq} + (4/3)\ O_2 \Leftrightarrow (16/3)\ \alpha\text{-}Fe^{III}OOH + (2/3)Fe^{3+} + 2H_2O + (1/3)\ H_2$$

$$5\ Fe^{II}(OH)_2 + Fe^{2+}_{aq} + (3/2)\ O_2 + 2\ OH^- \Leftrightarrow 6\ \alpha\text{-}Fe^{III}OOH + 3\ H_2O$$

The *in situ* oxidation of green rusts by deprotonation

Use a strong oxidant such as H_2O_2, Dry the green rust and oxide in the air, Violent air oxidation, Oxide in a basic medium…

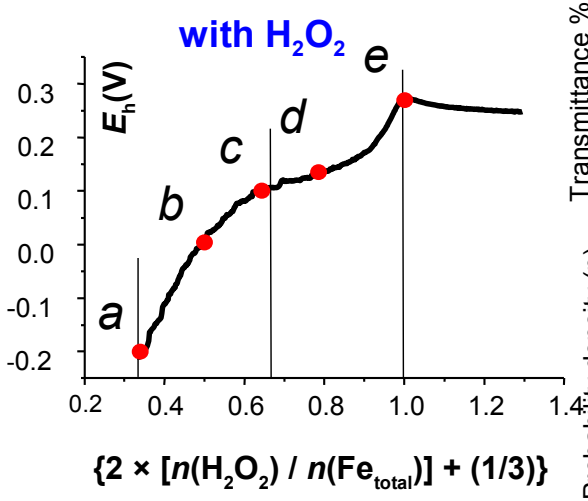

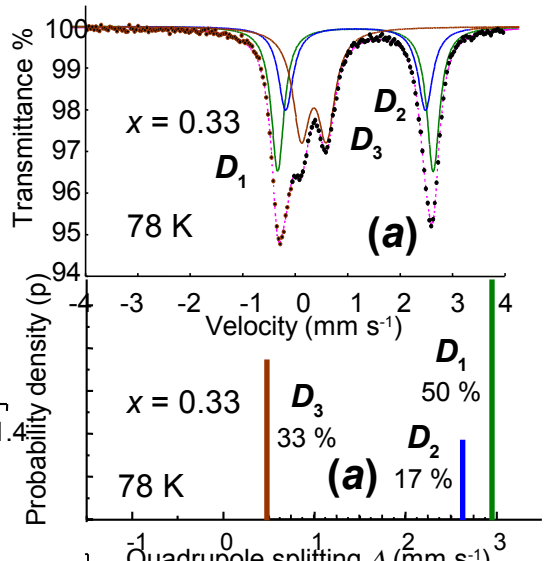

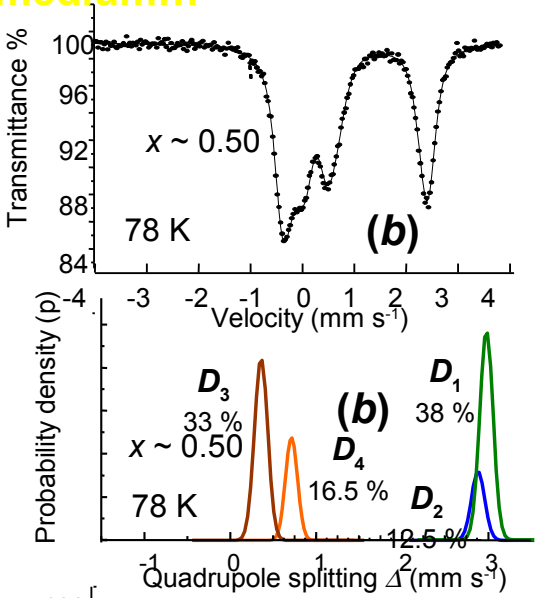

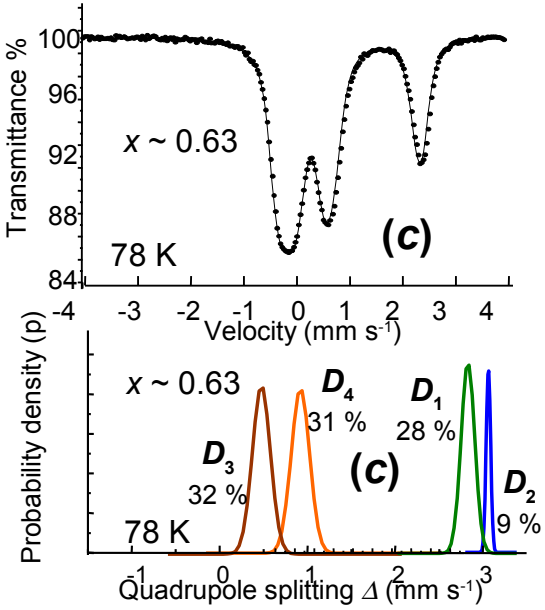

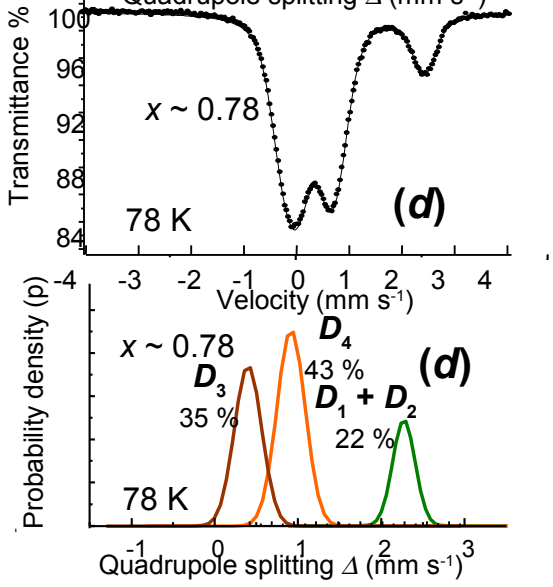

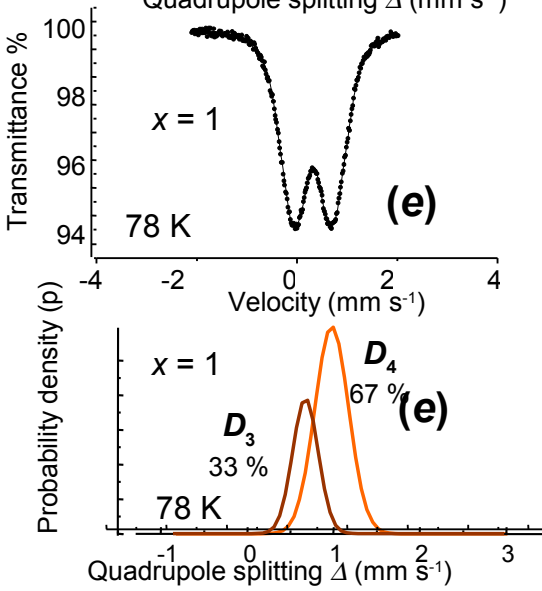

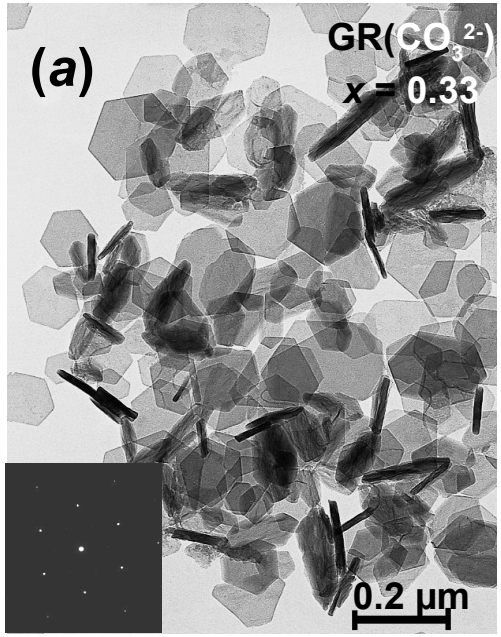

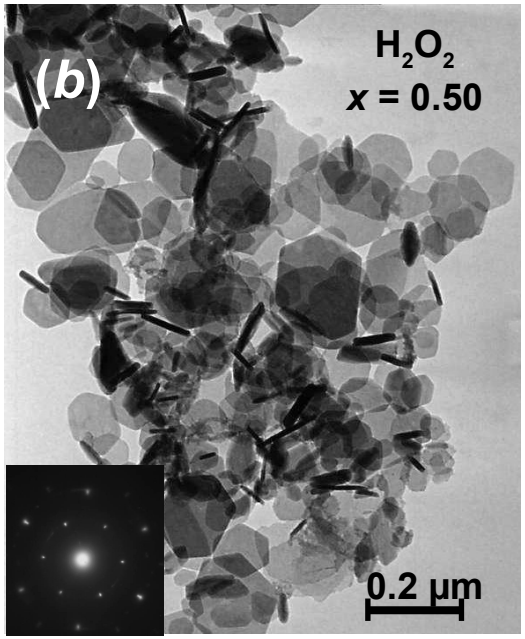

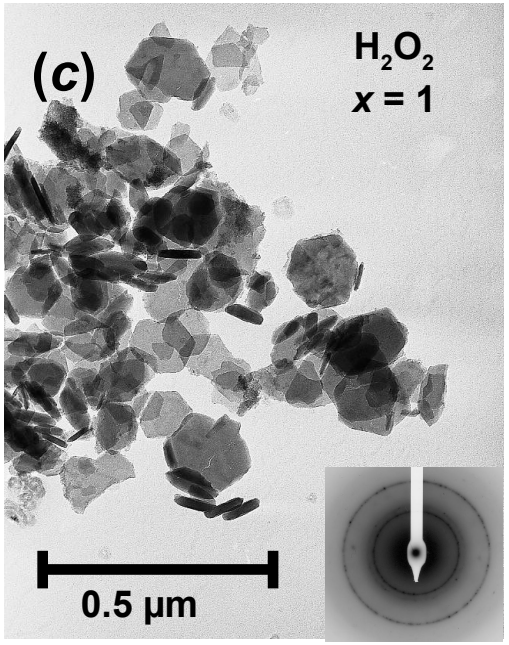

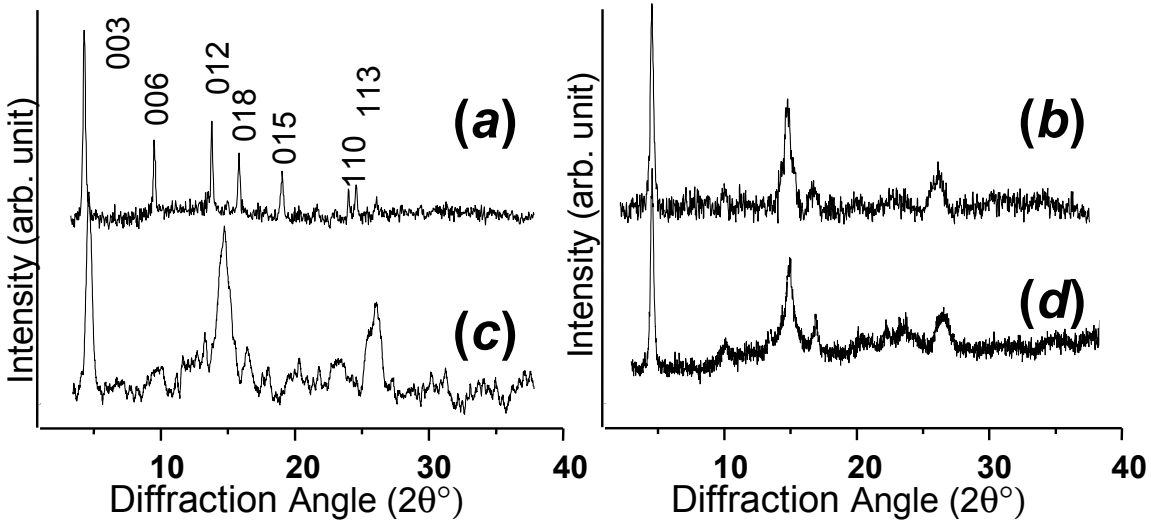

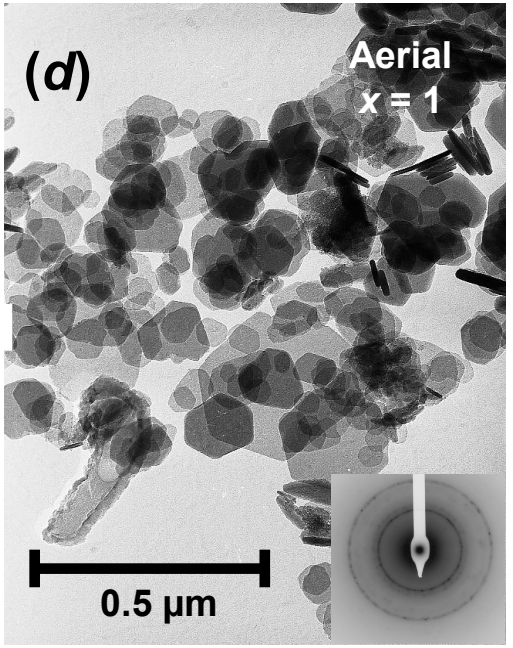

TEM and XRD patterns

The oxidation is in situ and does not destroy the cristals

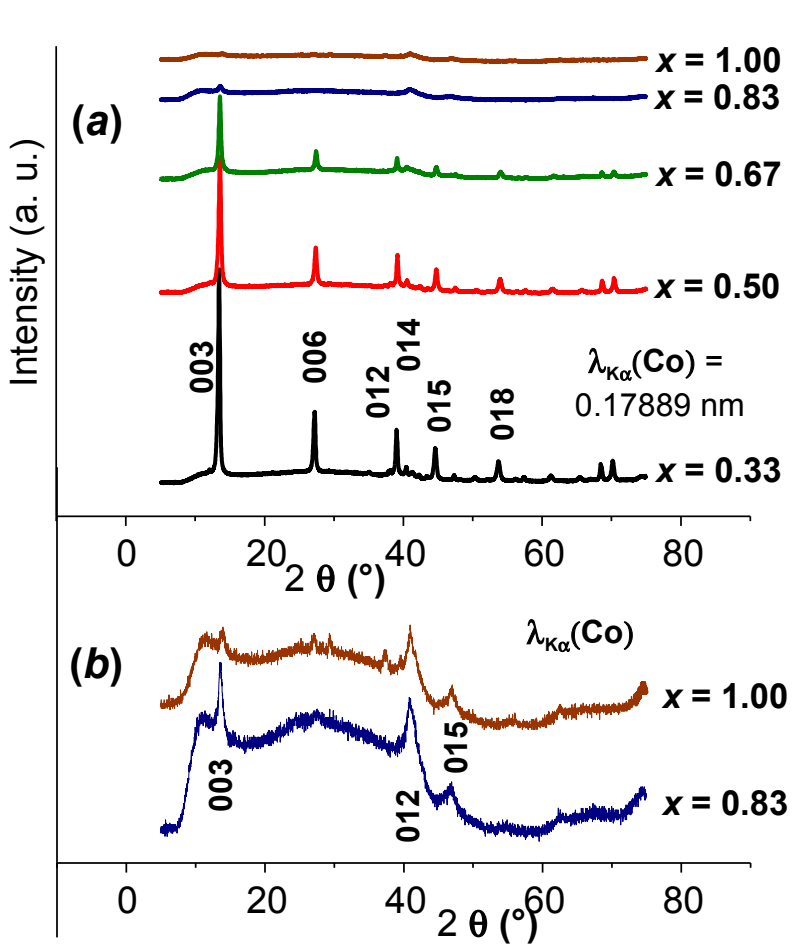

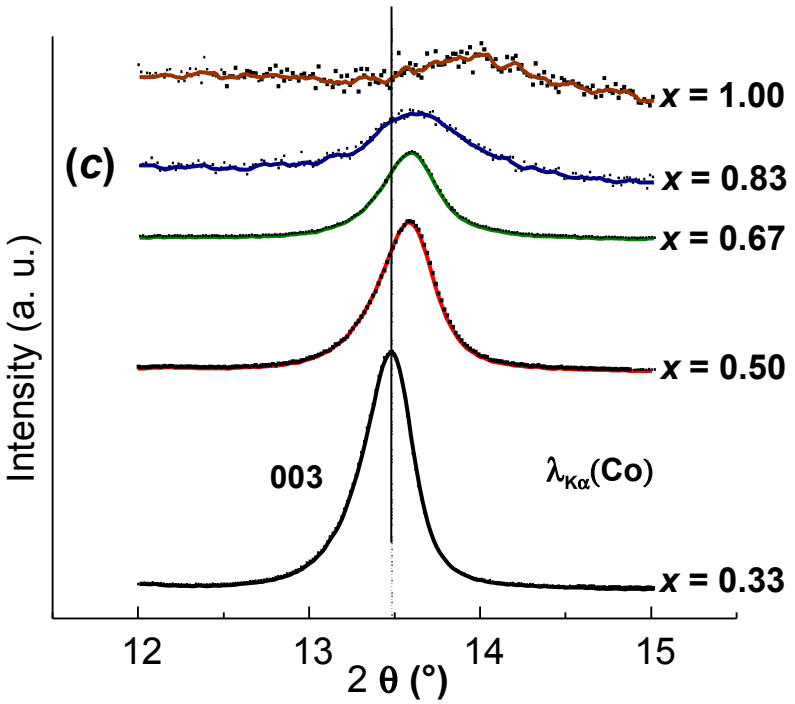

XRD patterns of the Fe^{II-III} oxyhydroxycarbonate with respect to $x = Fe^{III}/Fe_{total}$

G. Ona N'Guema

$$Fe^{II}_{6(1-x)}\ Fe^{III}_{6x}\ O_{12}H_{2(7-3x)}\ CO_3$$

Lines of ferric GR* (x=1) are very weak; this explains why its existence was not discovered sooner

The oxidation or reduction of $GR(CO_3^{2-})$ gives rise to $GR(CO_3^{2-})^*$ or $GR(CO_3^{2-})^{\S}$, i.e. $Fe^{II}_{6(1-x)}\ Fe^{III}_{6x}\ O_{12}\ H_{2(7-3x)}\ CO_3$ where $x \in [0, 1]$; the fougerite mineral is limited to the range [1/3, 2/3].

$$R = \{n_{OH^-} / (n_{Fe(II)} + n_{Fe(III)})\}$$

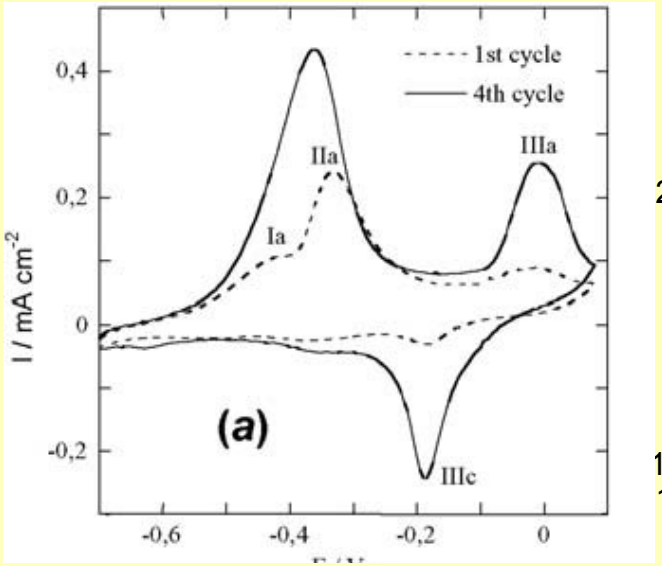

Voltammograms obtained on an iron disc at 10 mVs^{-1} in 0.4 M $NaHCO_3$ solution at 25 °C and pH = 9.6.

$$Fe^{II}_4Fe^{III}_2(OH)_{12}CO_3 + O_2 \rightarrow Fe^{III}_6O_{12}H_8CO_3 + 2\ H_2O$$

Mass balance diagram of iron compounds

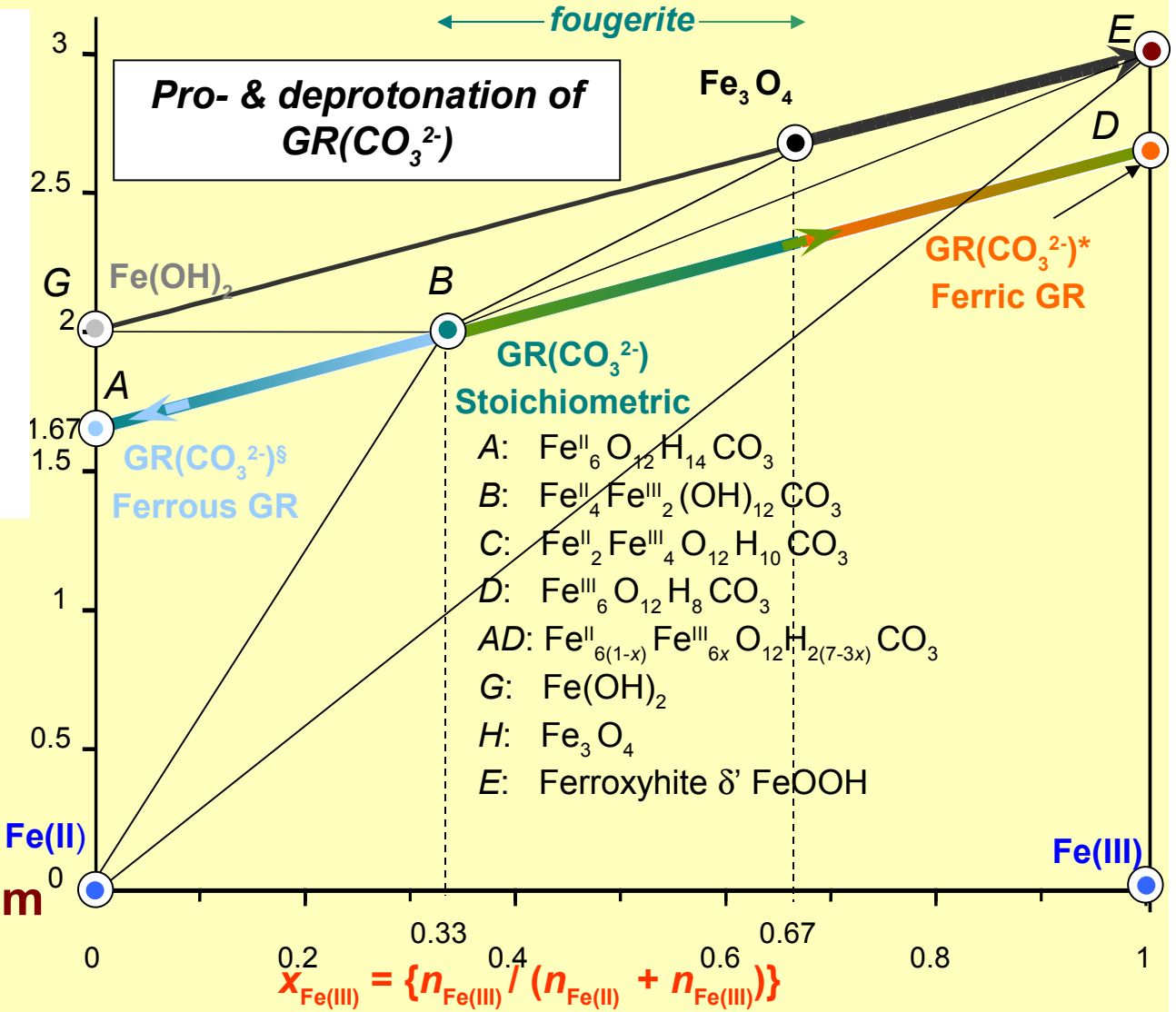

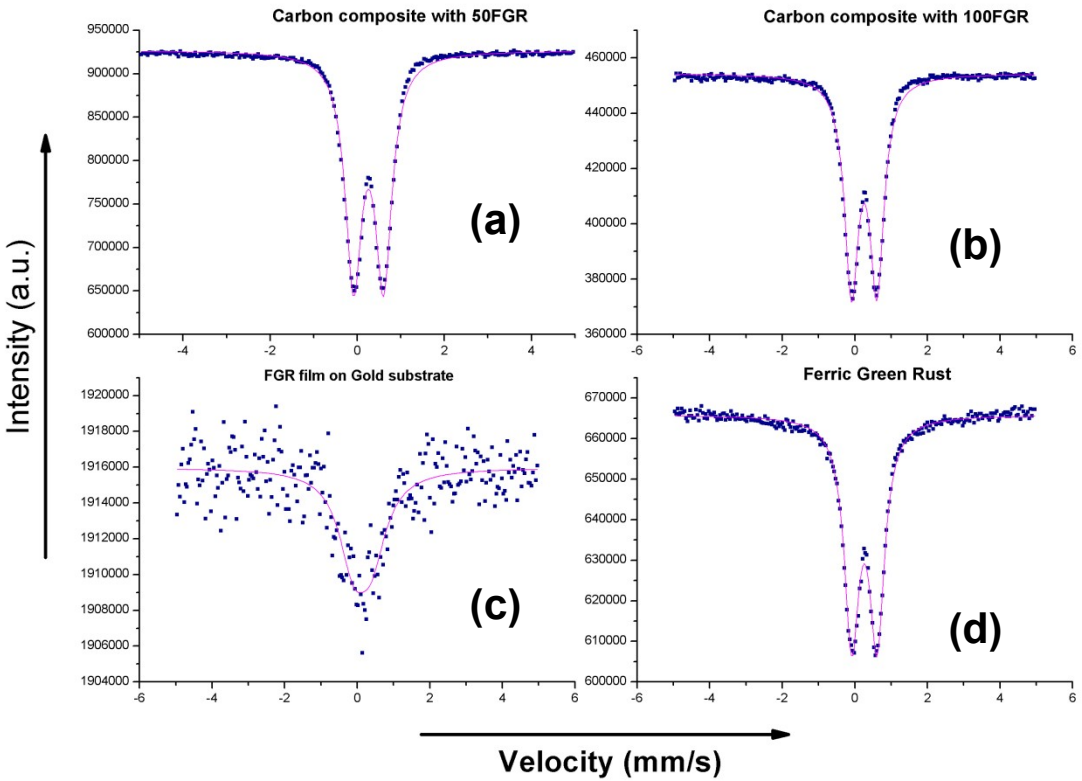

Comparative Mössbauer spectra for
(b) 50 mg ferric green rust in graphite
(b) 100 mg ferric green rust in graphite
(c) thin film of ferric green rust on gold
(d) Reference ferric green rust

$$Fe^{II}_{6(1-x)}\ Fe^{III}_{6x}\ O_{12}\ H_{2(7-3x)}\ CO_3$$

$$x \in [0 - 1]$$

Voltammetry

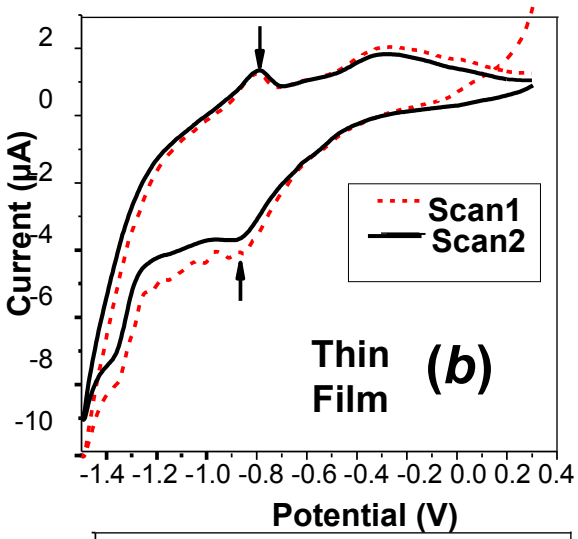

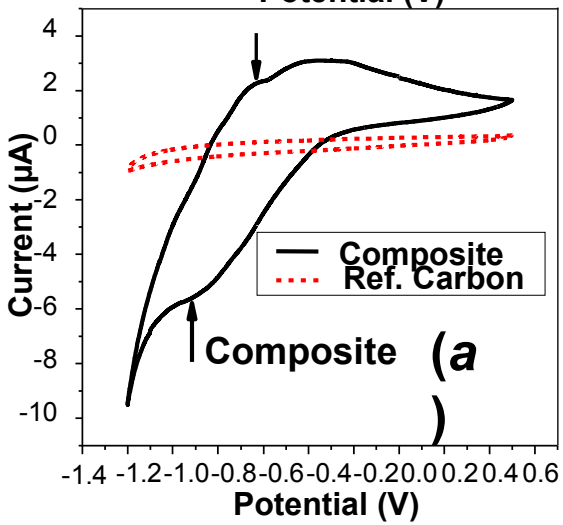

Three sublattices

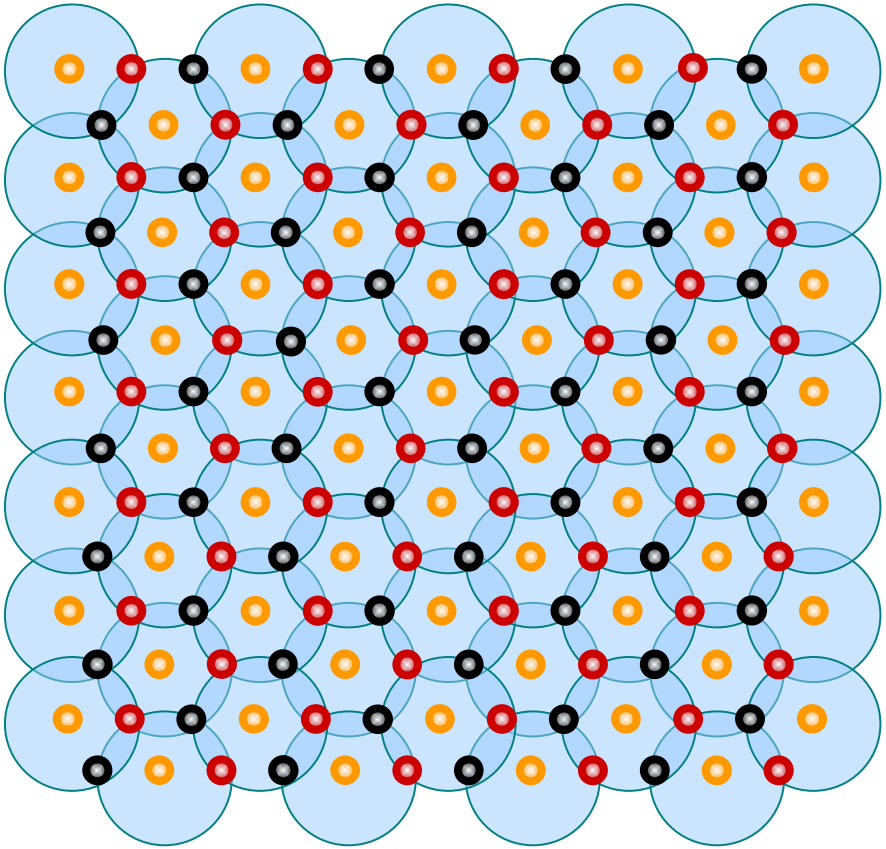

1st lattice
2nd lattice
3rd lattice

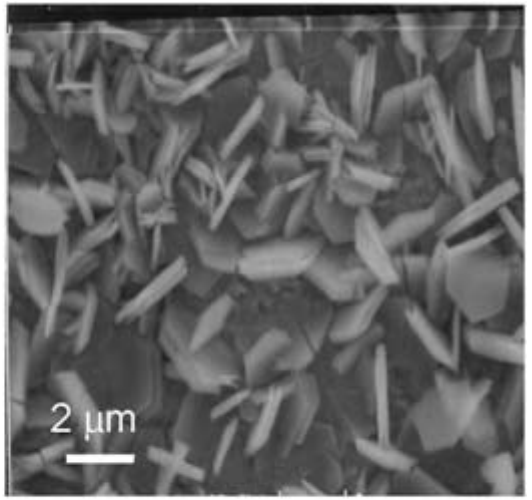

SEM image of the orange ferric compound resulting from the oxidation by air of electrochemically formed GR1(CO_3^{2-})* after ageing at 30 °C for 50 days.

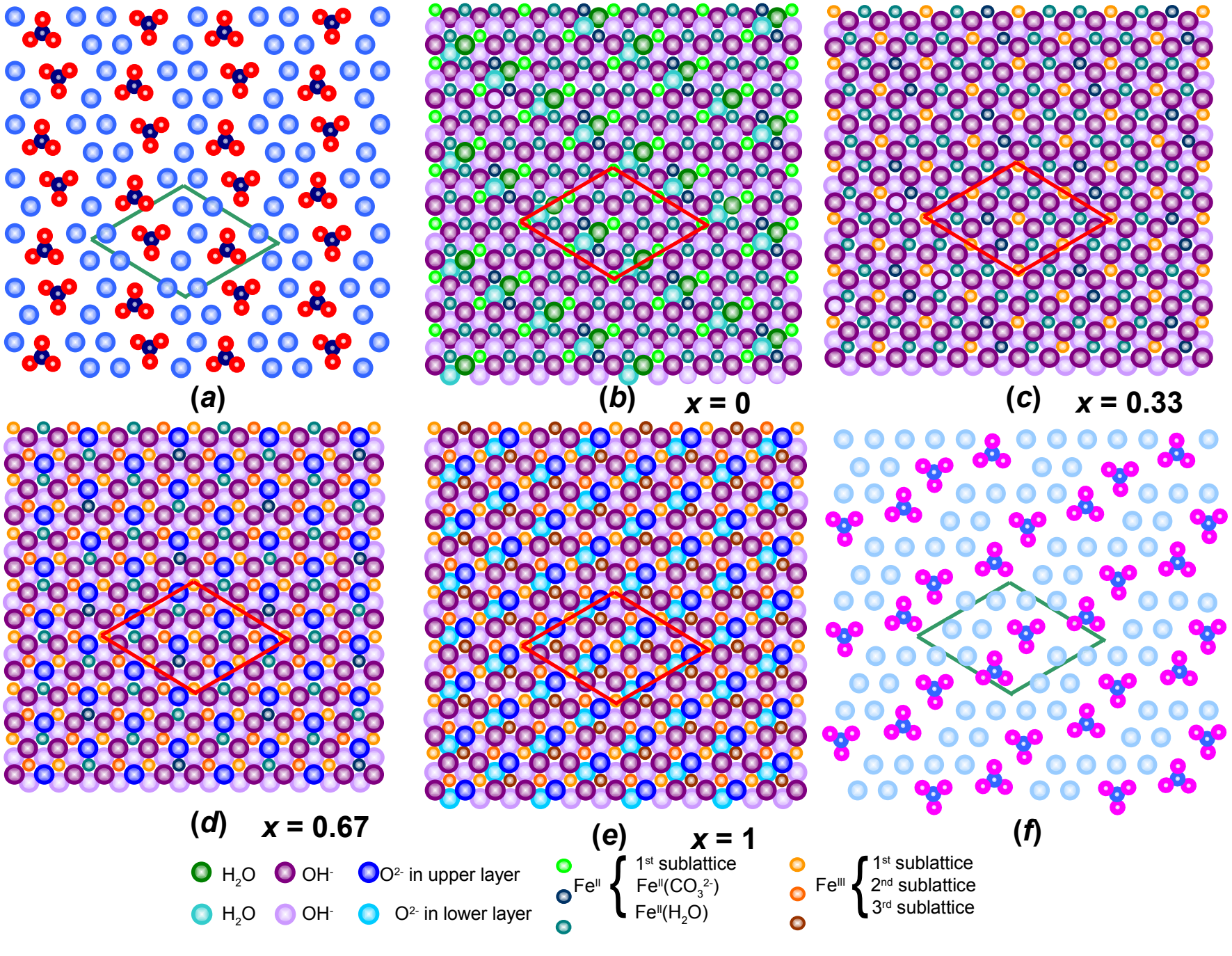
(a)
(b) x = 0
(c) x = 0.33
(d) x = 0.67
(e) x = 1
(f)
H2O
OH-
O2- in upper layer
H2O
OH-
O2- in lower layer
FeII
1st sublattice
FeII(CO3 2-)
FeII(H2O)
FeIII
1st sublattice
2nd sublattice
3rd sublattice

Fe^{II-III} oxyhydroxycarbonate

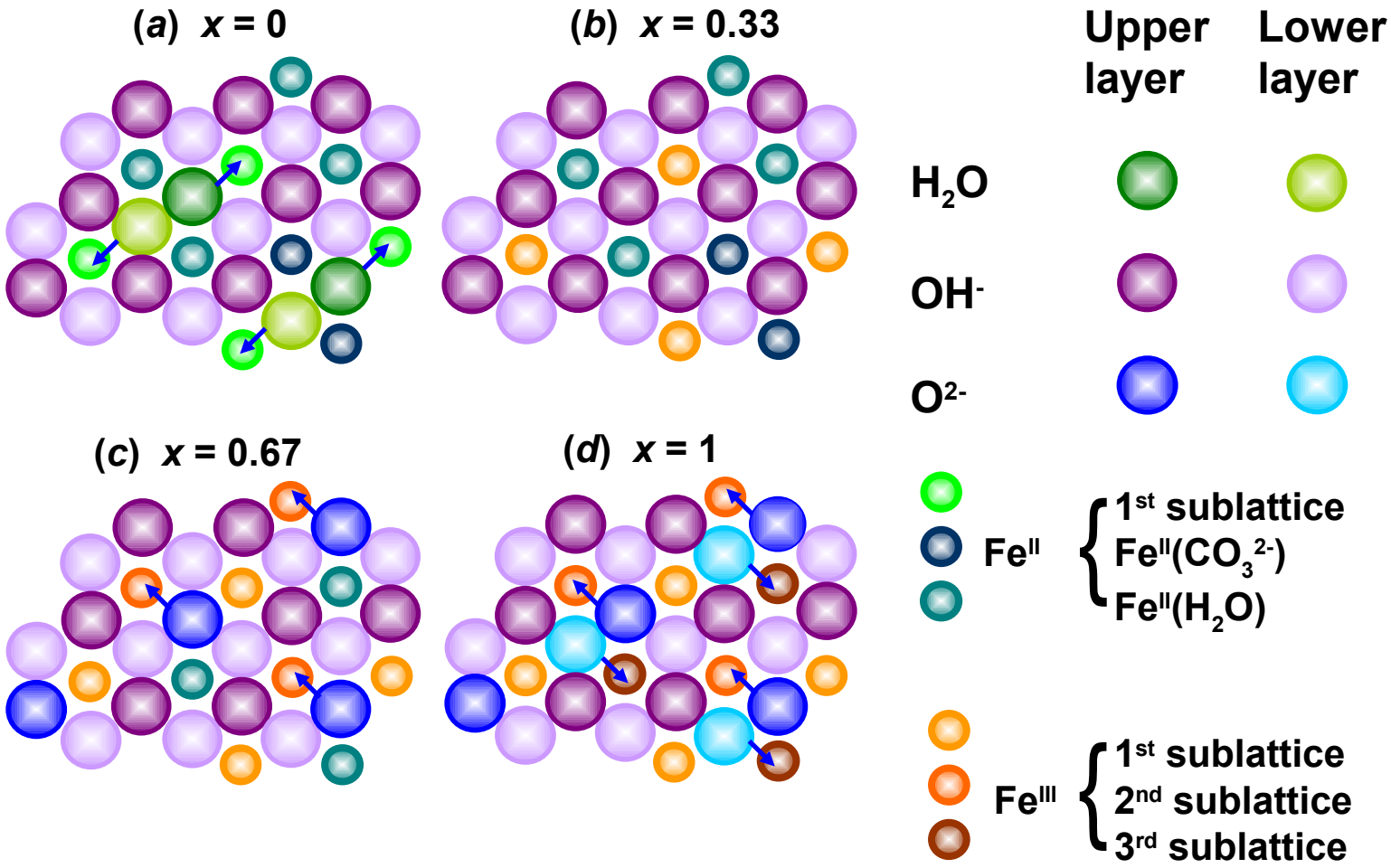

$Fe^{II}_{6(1-x)}\ Fe^{III}_{6x}\ O_{12}\ H_{2(7-3x)}\ CO_3$

Protonation and deprotonation of OH- ions

$Fe^{II}_4\ Fe^{III}_2\ (OH)_{12}\ CO_3$ ferrimagnetism

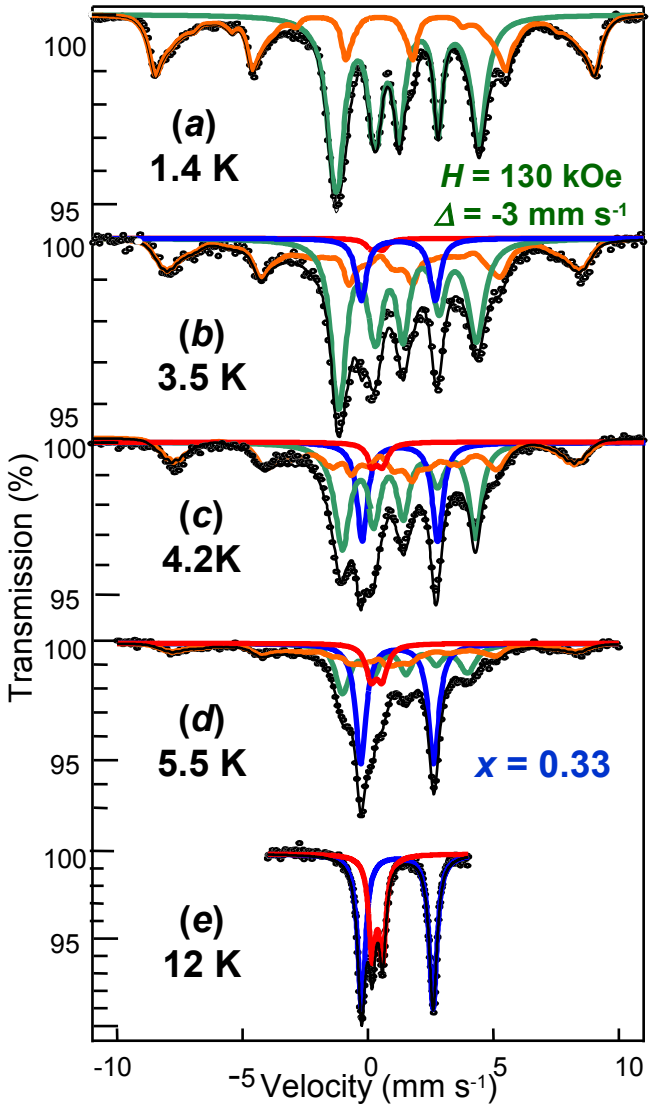

- **Evolution of Mössbauer spectra with measurement temperature displaying the ferrimagnetic behaviour of stoichiometric GR(CO_3^{2-}) between 1.4 and 12 K.**

$Fe^{III}_6\ O_{12}\ H_8\ CO_3$ ferromagnetism

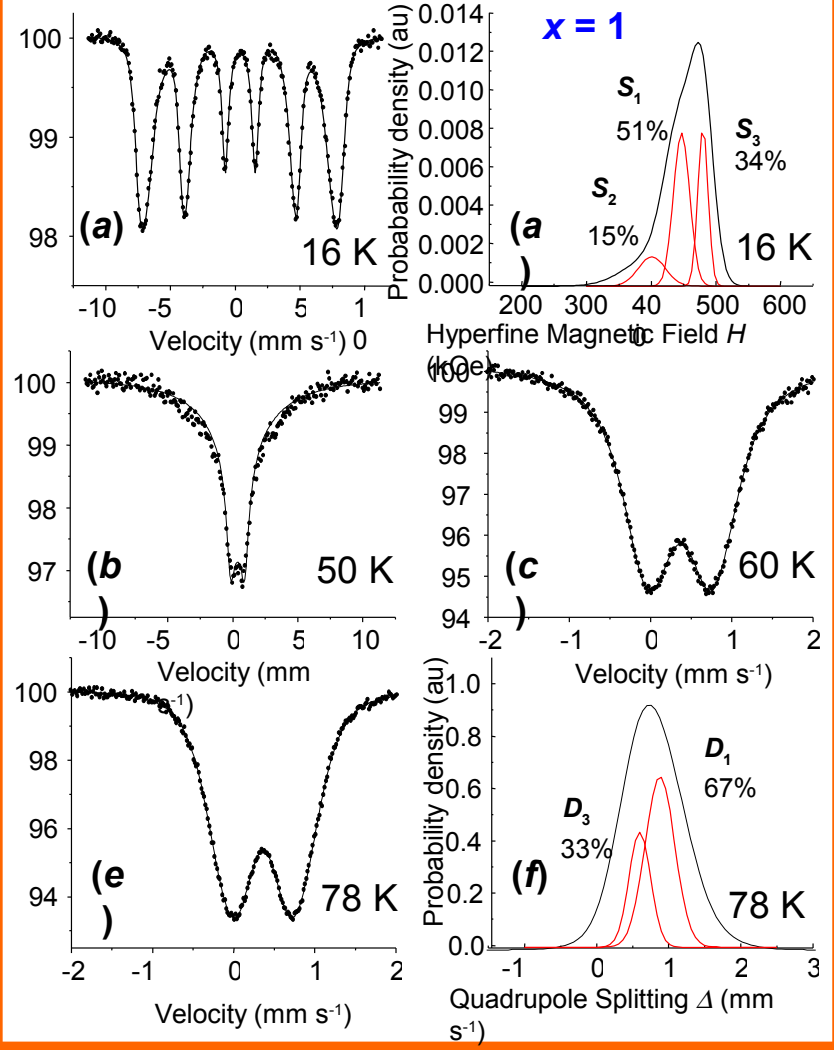

Mössbauer spectra of GR(CO_3^{2-}) sample oxidised violently by H_2O_2 and named ferric [GR(CO_3^{2-})*]$_1$. Measurement temperatures are (a) 16 K, (c) 50 K, (d) 60 K and (e) 78 K. (b) and (f) are the hyperfine field distribution of (a) and quadrupole splitting distribution of (e) using a Voigt profile analysis, respectively.

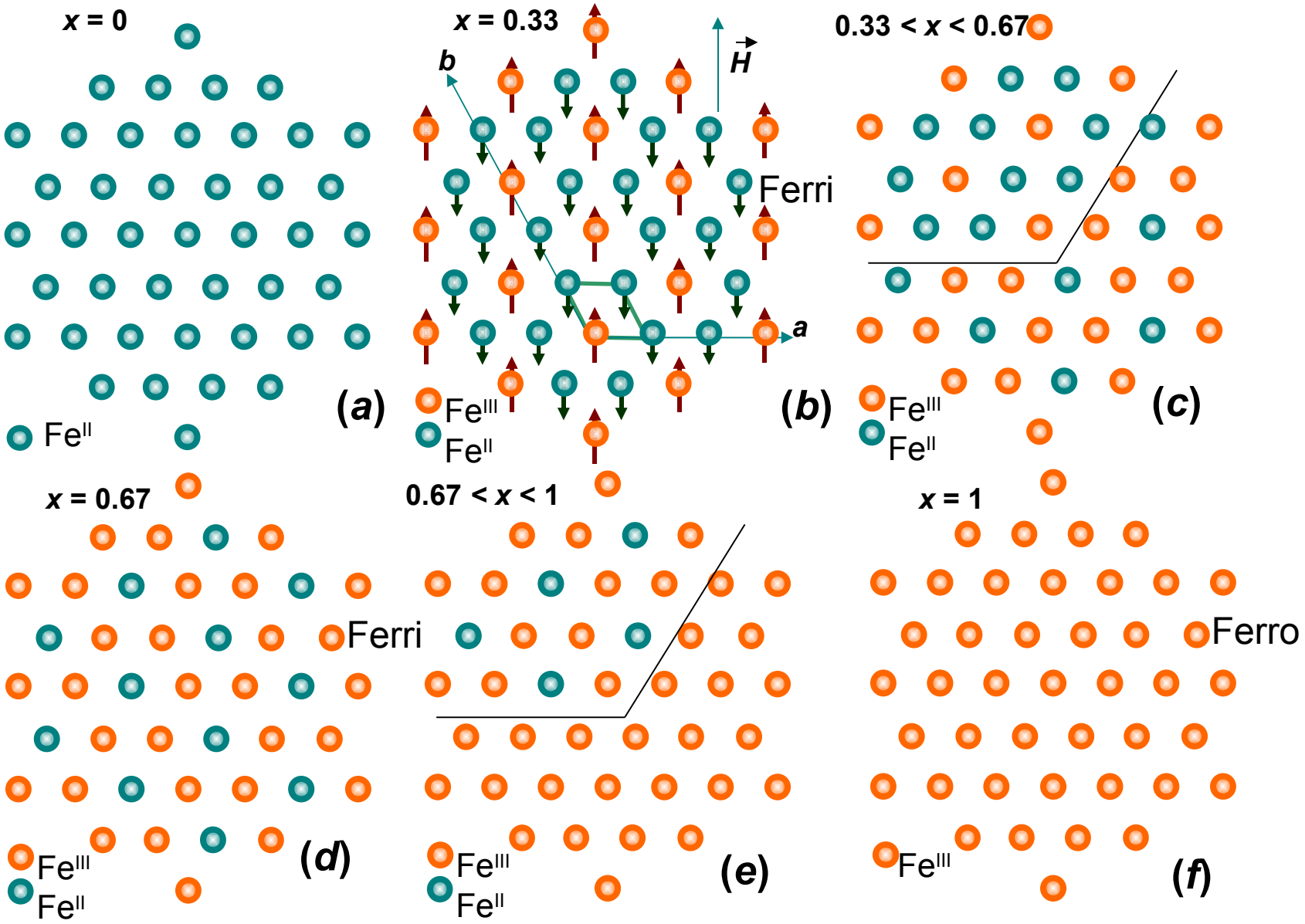

Hexagonal pavements of Fe^{II} and Fe^{III} cations in the layers of (a) $Fe(OH)_2$, (b) stoichiometric $GR(CO_3^{2-})$ at $x = 1/3$, (c) $GR(CO_3^{2-})$* with $1/3 < x < 2/3$, (d) $GR(CO_3^{2-})$* at $x = 2/3$, (e) $GR(CO_3^{2-})$* with $2/3 < x < 1$ and (f) fully ferric $GR(CO_3^{2-})$* at $x = 1$. Long range order is displayed showing magnetic domains

Aqueous corrosion of iron

Fe0 — ***Iron, Steels***

↓

Fe^{II} — ***Ferrous hydroxide***

↓

Agressive anions (Cl^-, CO_3^{2-}, SO_4^{2-})

Fe^{II-III} — ***Green rusts***

Dissolution-precipitation	***In situ* deprotonation**
↓	↓

Fe^{III} ***Common rusts*** — ***Ferric green rust***

Including anions

Goethite **Magnetite**
Lepidocrocite **Akaganeite**
δFeOOH **Ferroxyhite**

The secret of passivation of steel is understood

POURBAIX diagrams of iron and water

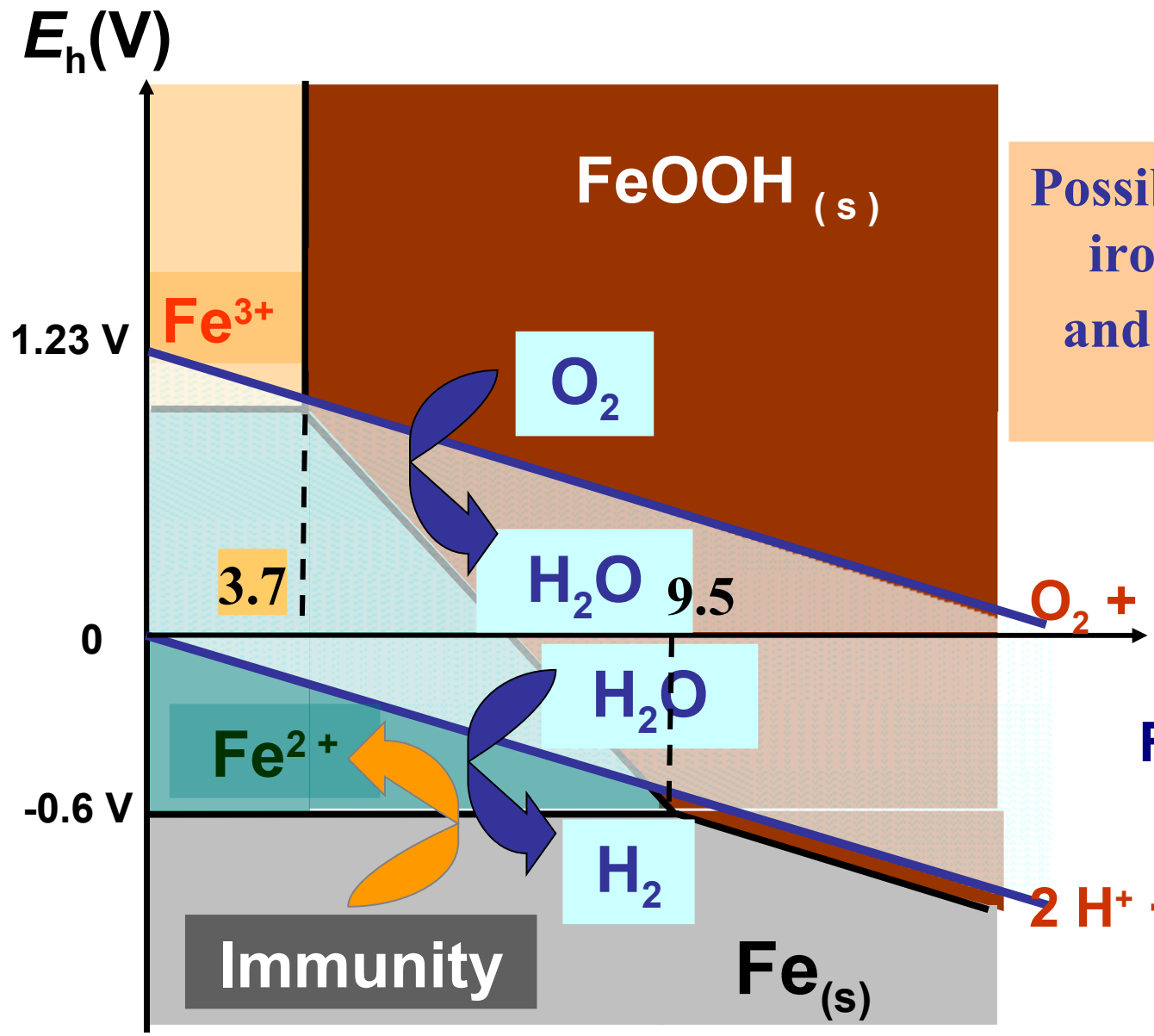

Possibility of oxidation of iron by dissolved O_2 and by water mainly in acidic medium

$O_2 + 4H^+ + 4\ e^- \Rightarrow 2\ H_2O$

$Fe^0 \Rightarrow Fe^{2+} + 2\ e^-$

$2\ H^+ + 2\ e^- \Rightarrow H_2$

From the atlas by Marcel Pourbaix

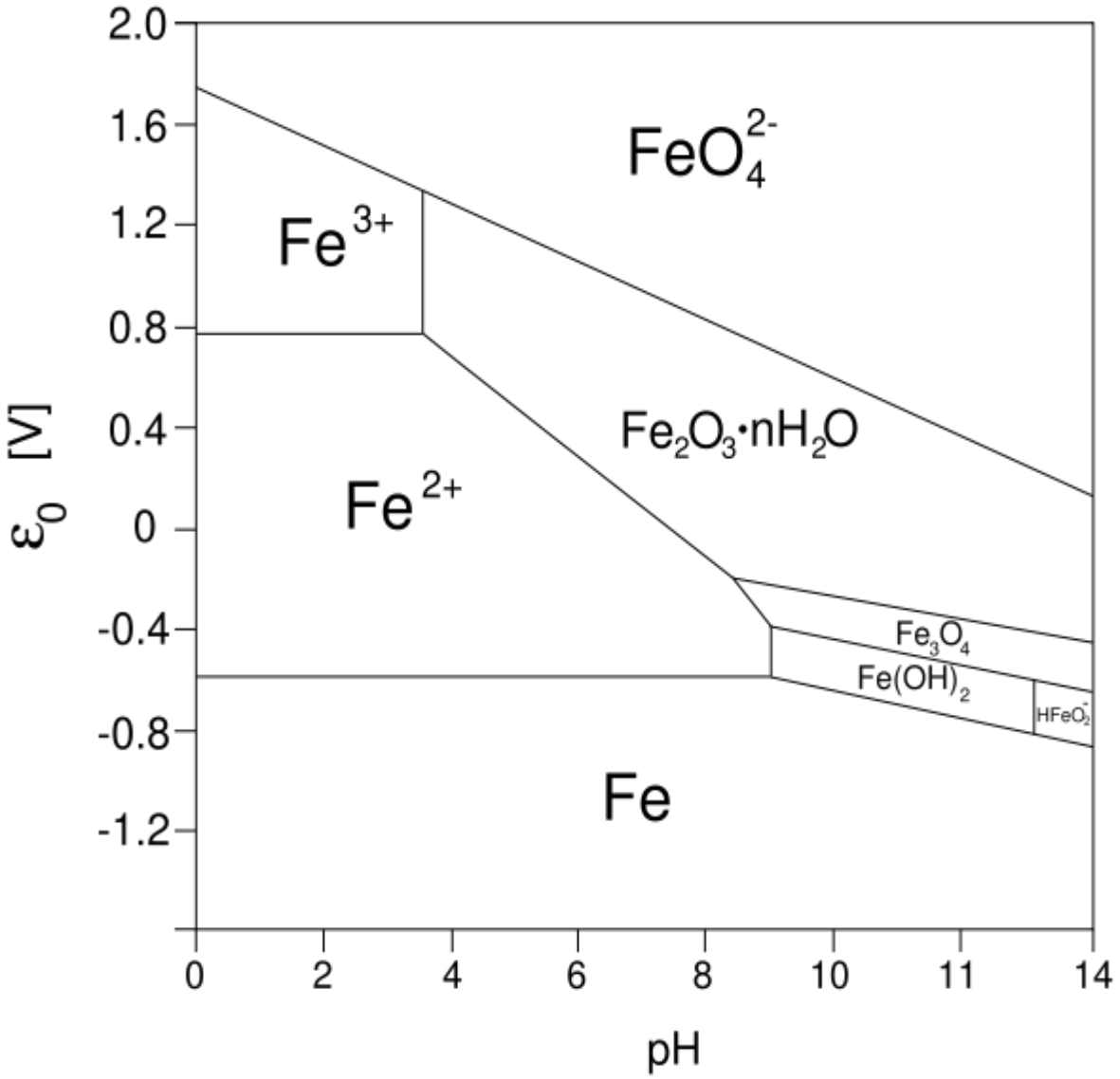

Marcel Pourbaix
1904-1998

How to complete the Pourbaix diagram of iron with the domains of green rusts?

Corrosion in chlorinated medium

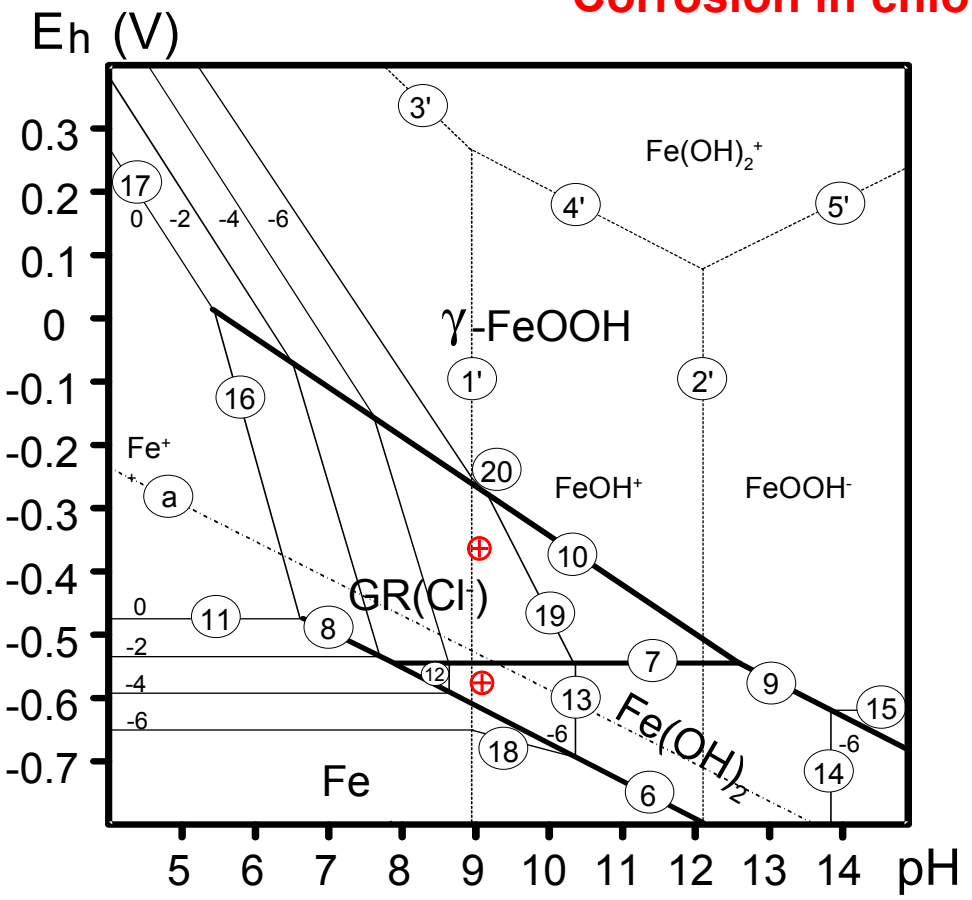

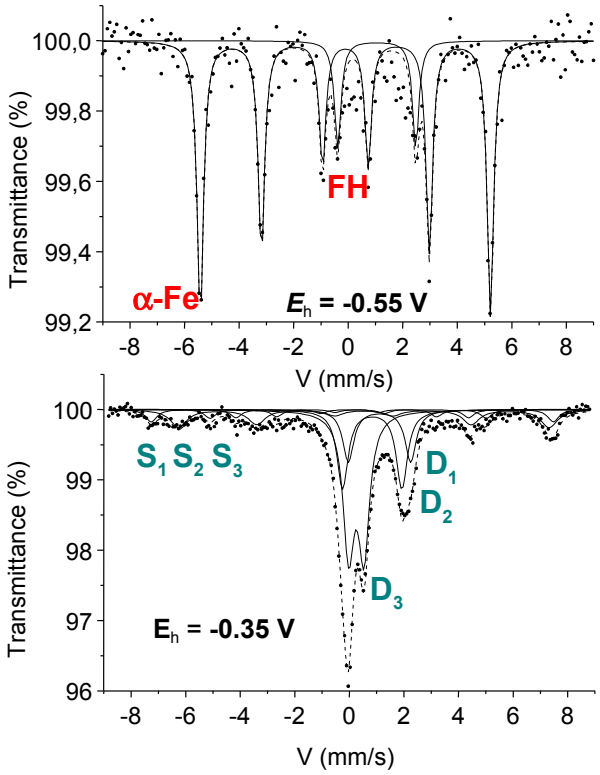

Pourbaix diagram of the Fe - H_2O - Cl^- system at 25 °C for a [Cl^-] activity of 0.55 and *in situ* Mössbauer spectra of corrosion products of corrosion of an α-iron foil obtained at E_h = -0.55 V and -0.35 V at pH = 9 in an electrochemical cell.
⊕ experimental conditions.

***D_1*, *D_2* and *D_3* are doublets of green rusts, *FH* is that of $Fe(OH)_2$ and *S_1*, *S_2* et *S_3* are sextets due to magnetite and goethite.**

[Ph. Refait, M. Abdelmoula & J.-M. Génin, Corros. Sci. 40 (1998) 1547].

• The first step of corrosion: the green rust layer

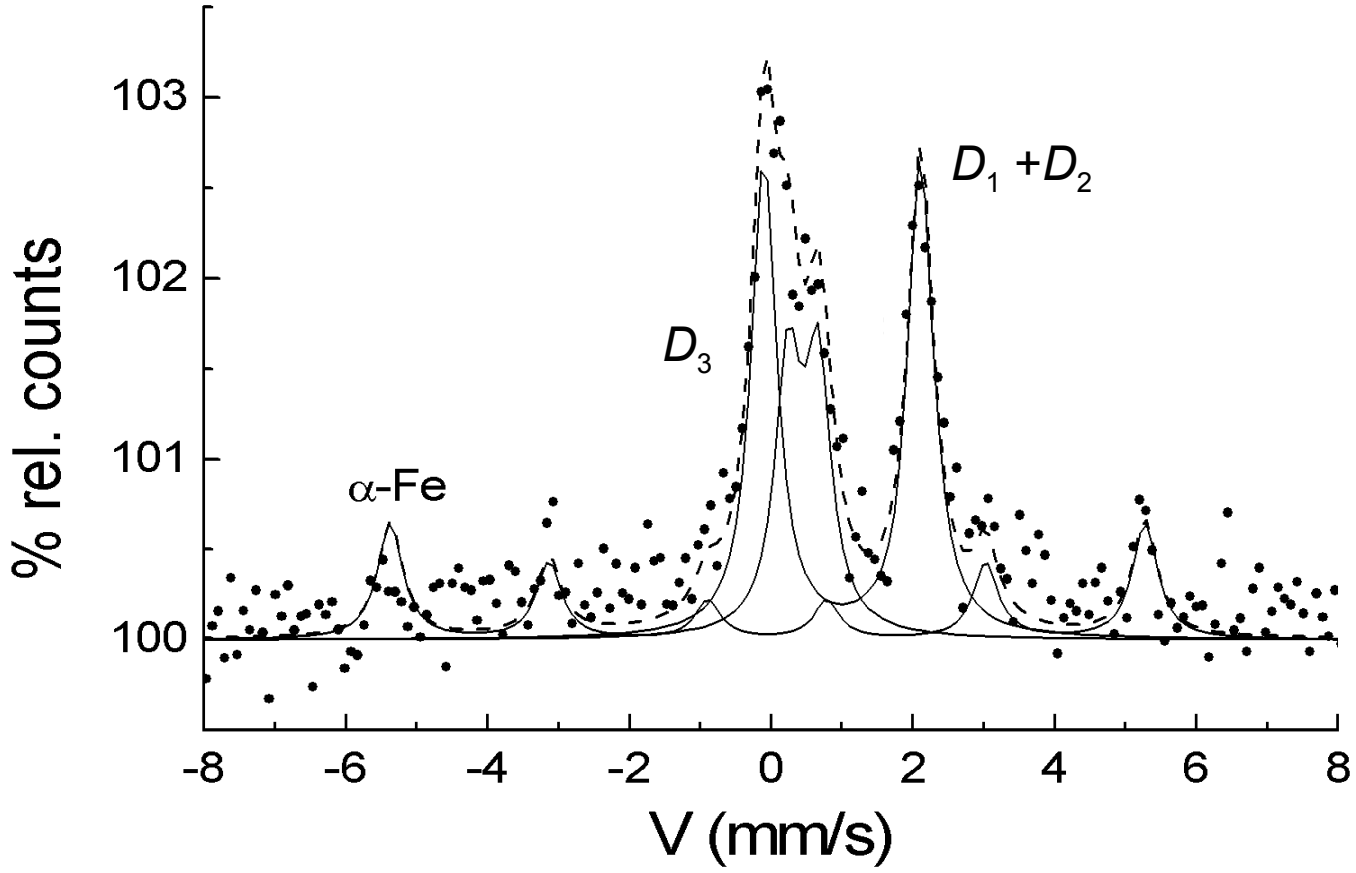

CEMS spectrum at room temperature of a steel disk dipped 24 hours in a 0.1 M $NaHCO_3$ solution. • • • : experimental curve, - - - : global computed curve. ____ : components of the spectra.

E_h-pH Pourbaix diagram of the Fe^{II-III} oxyhydroxycarbonate

Nerns' law

The new rust *In situ* deprotonation of GR1(CO_3^{2-})

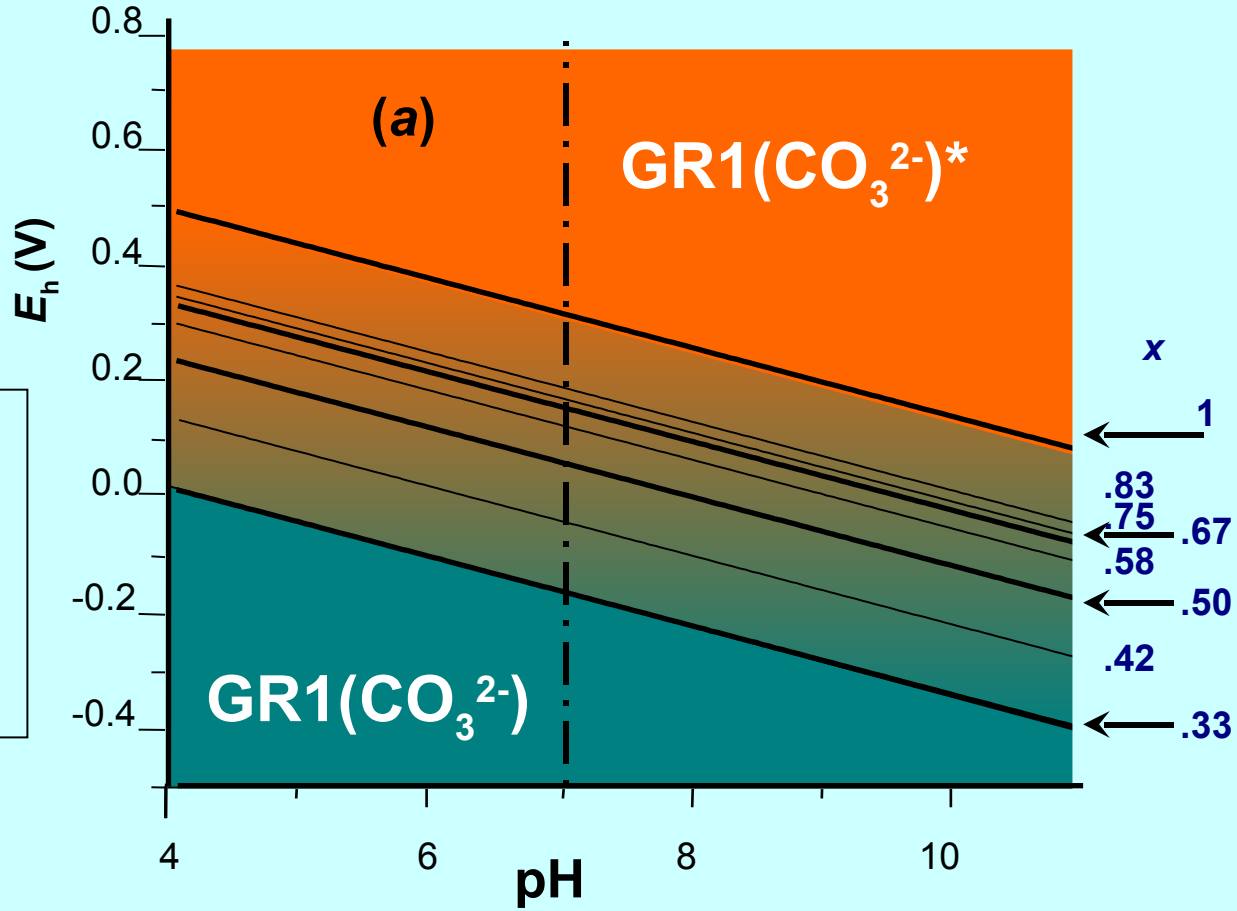

$$Fe^{II}_{6[1-(x+dx)]}\,Fe^{III}_{6(x+dx)}\,O_{12}\,H_{2[7-3(x+dx)]}\,CO_3 + (6\times dx)\,H^+ + (6\times dx)\,e^- \rightarrow Fe^{II}_{6(1-x)}\,Fe^{III}_{6x}\,O_{12}\,H_{2(7-3x)}\,CO_3$$

$$GR^*(x+dx) + dx\,H^+ + dx\,e^- \rightarrow GR^*(x)$$

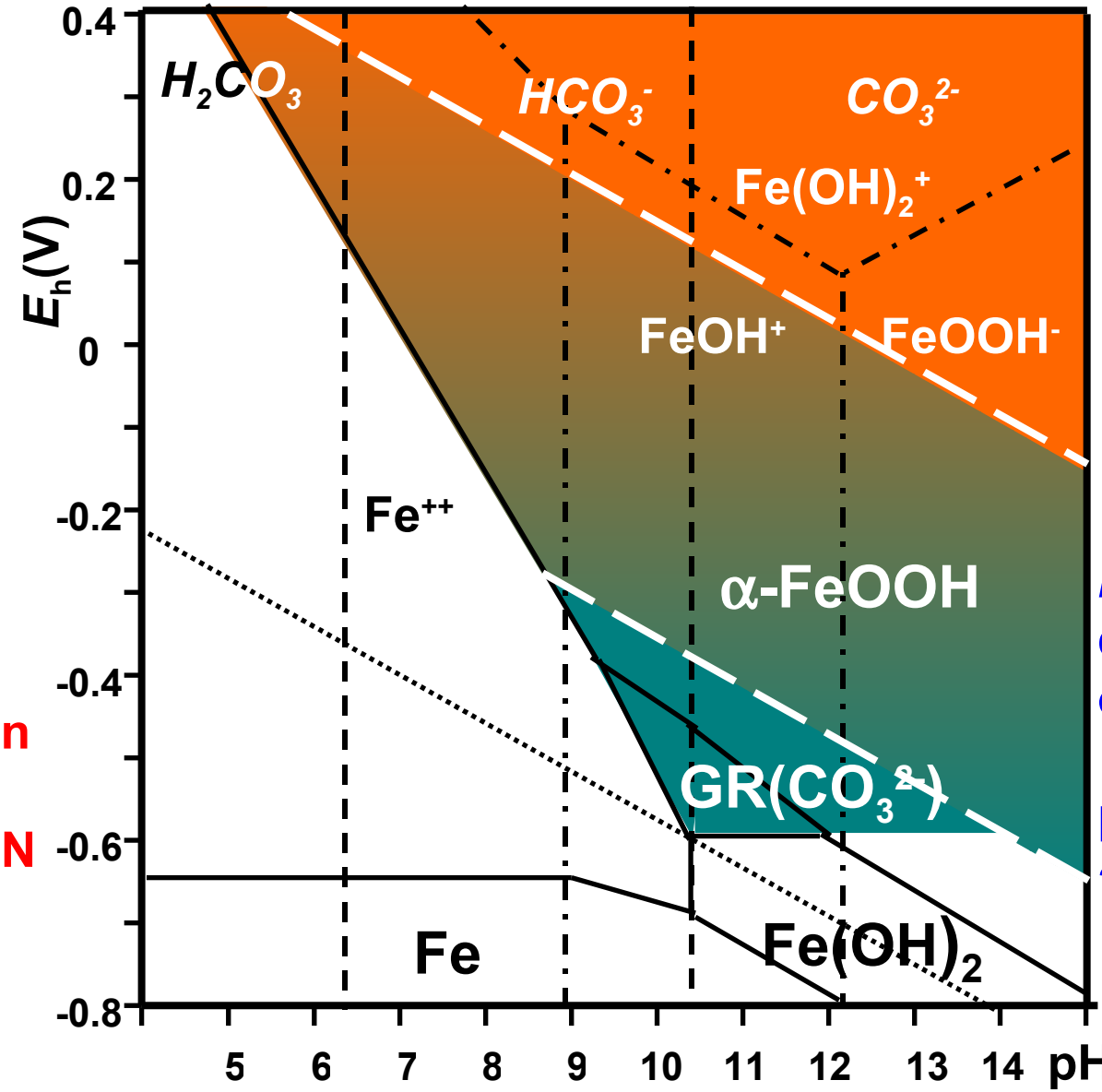

Dissolution and Precipitation

CORROSION

***In situ* deprotonation of GR1(CO_3^{2-})**

PASSIVATION ???????????

[Fe^{2+}] is 10^{-6} M

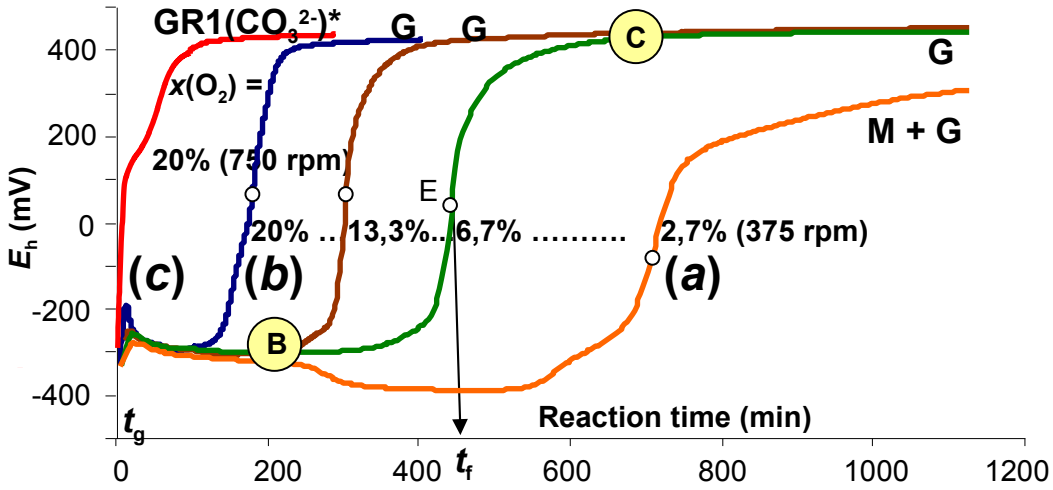

Oxidation by oxygen

(a) & (b) Dissolution-precipitation

- $Fe^{II}_4Fe^{III}_2(OH)_{12}\,CO_3 + 3/4\ O_2 \rightarrow 5\ Fe^{III}OOH + CO_3^{2-} + Fe^{2+} + 7/2\ H_2O$

(2) $Fe^{II}_4Fe^{III}_2(OH)_{12}\,CO_3 + 1/3\ O_2 \rightarrow 5/3\ Fe^{II}Fe^{III}_2\,O_4 + CO_3^{2-} + Fe^{2+} + 6\ H_2O$

(c) *In situ* deprotonation

(3) $Fe^{II}_4Fe^{III}_2(OH)_{12}CO_3 + O_2 \rightarrow Fe^{III}_6O_{12}H_8CO_3 + 2\ H_2O$

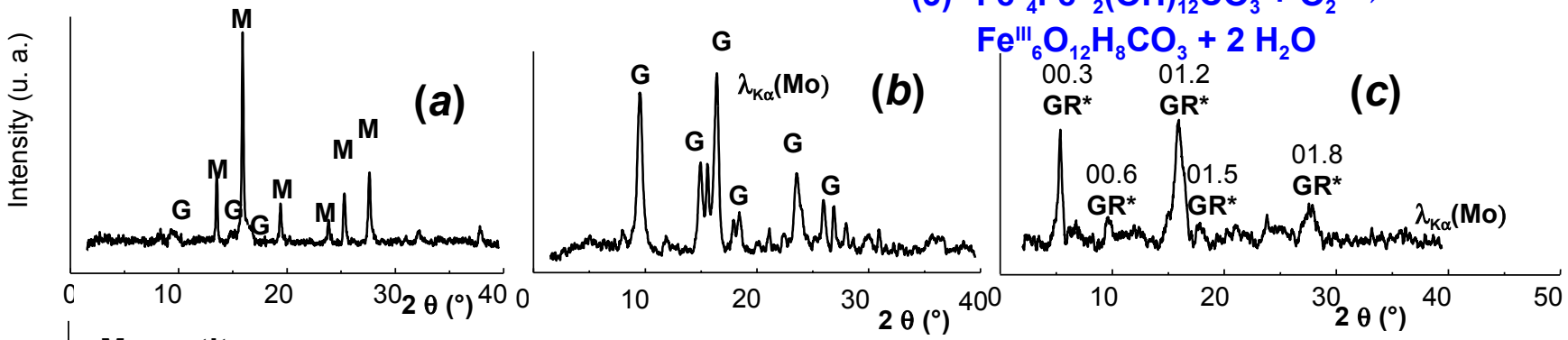

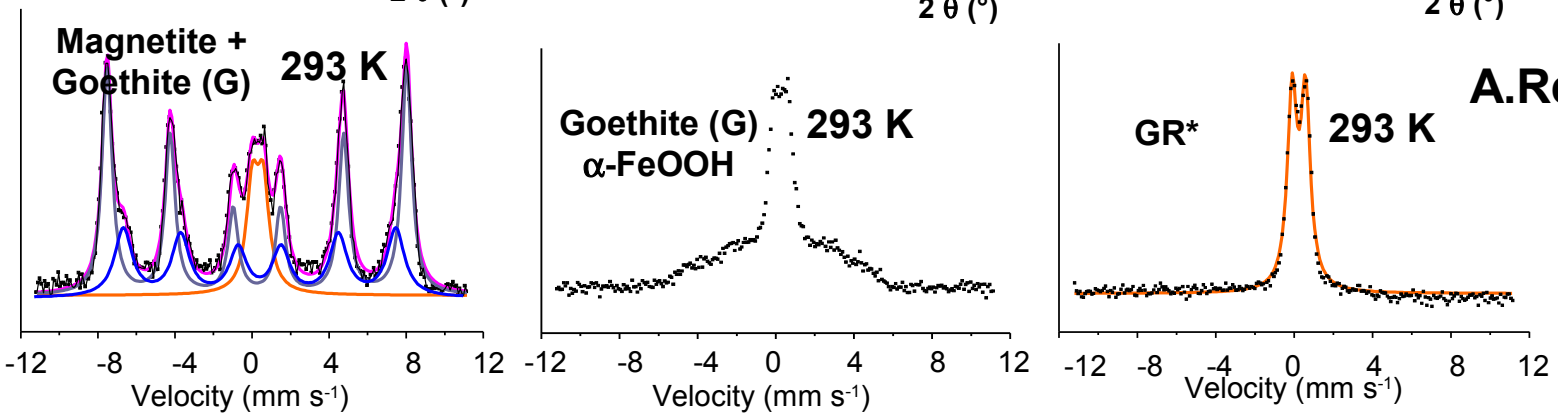

Bacterial reduction

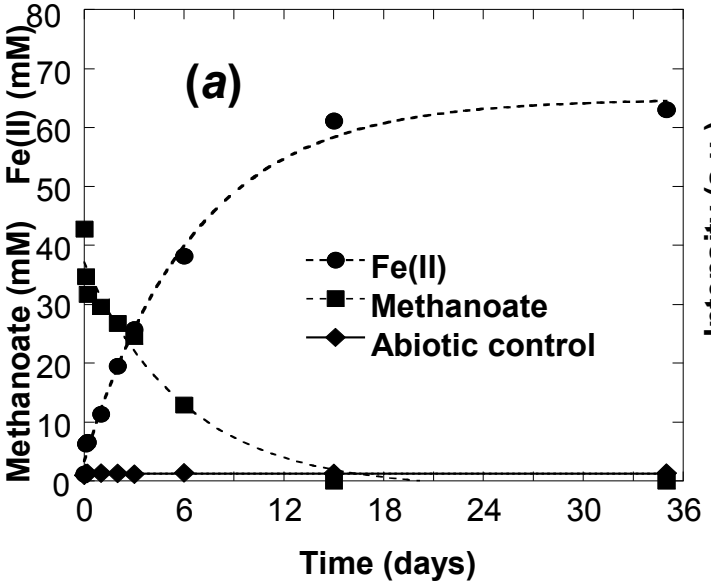

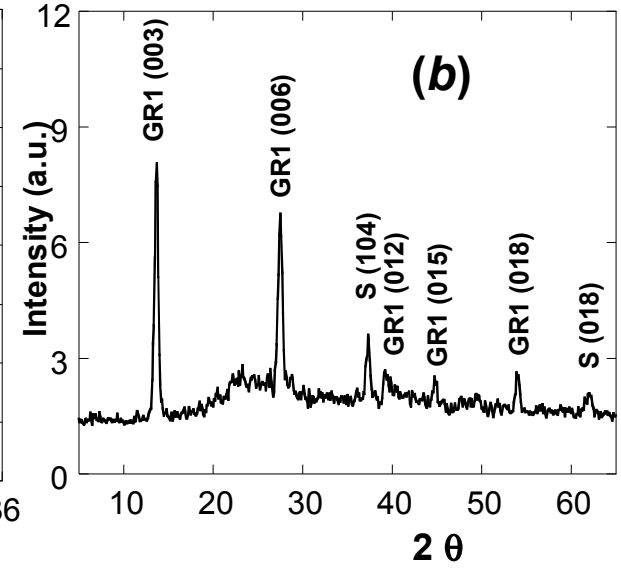

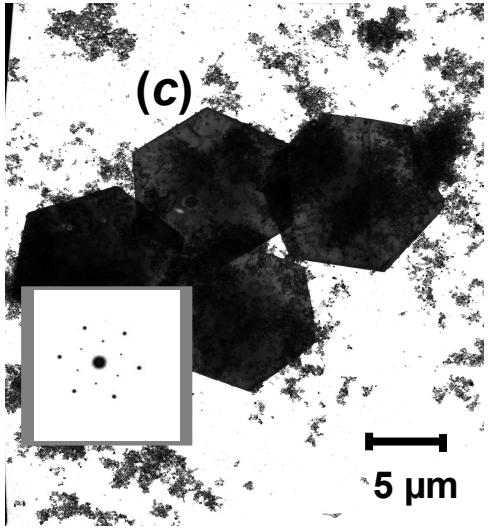

Georges Ona-Nguema

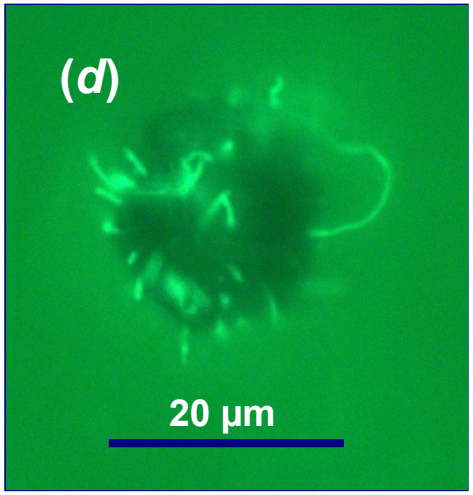

Asfaw Zegeye

- Production of Fe(II) and consumption of methanoate during culture of *Shewanella putrefaciens* in presence of lepidocrocite. The initial amount of Fe^{III} (as lepidocrocite) and of methanoate were respectively 80 mM and 43 Mm.
- (b) X-ray pattern of the solid phase of incubation experiments with *S. putrefaciens*: mixture of green rust (GR1) and siderite (S) obtained after 15 days of incubation

(c) TEM observations and

(d) optical micrograph of GR crystals obtained by reduction of lepidocrocite by *S. putrefaciens*; One sees the bacteria that respirate GR*.

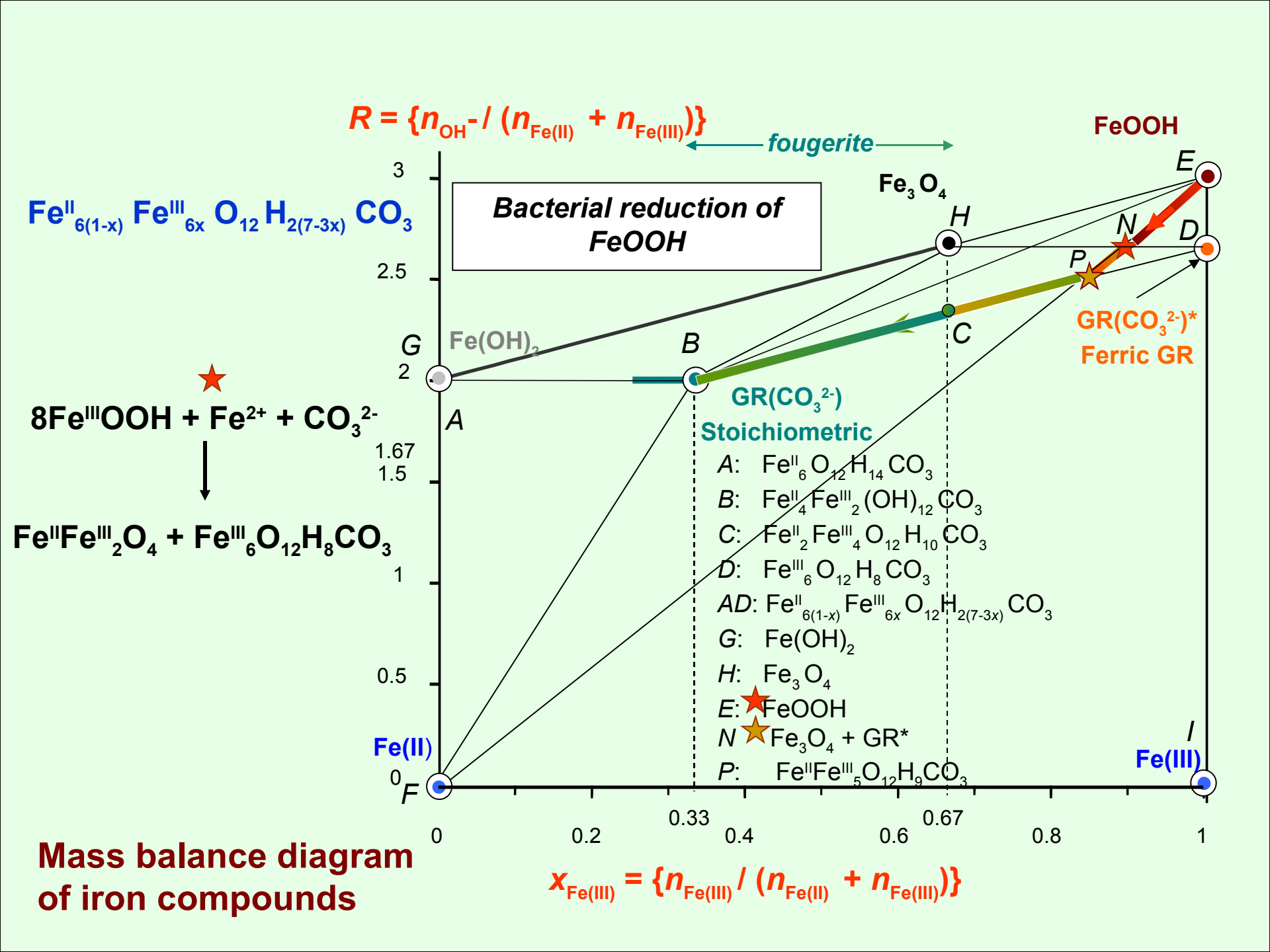
$R = \{n_{OH^-} / (n_{Fe(II)} + n_{Fe(III)})\}$
fougerite
FeOOH
$Fe^{II}_{6(1-x)}\ Fe^{III}_{6x}\ O_{12}\ H_{2(7-3x)}\ CO_3$
Bacterial reduction of FeOOH
Fe_3O_4
E
H
N
D
P
$GR(CO_3^{2-})$*
Ferric GR
C
B
G
$Fe(OH)_2$
$GR(CO_3^{2-})$
Stoichiometric
A
$8Fe^{III}OOH + Fe^{2+} + CO_3^{2-}$
$Fe^{II}Fe^{III}_2O_4 + Fe^{III}_6O_{12}H_8CO_3$
A: $Fe^{II}_6O_{12}H_{14}CO_3$
B: $Fe^{II}_4Fe^{III}_2(OH)_{12}CO_3$
C: $Fe^{II}_2Fe^{III}_4O_{12}H_{10}CO_3$
D: $Fe^{III}_6O_{12}H_8CO_3$
AD: $Fe^{II}_{6(1-x)}Fe^{III}_{6x}O_{12}H_{2(7-3x)}CO_3$
G: $Fe(OH)_2$
H: Fe_3O_4
E: FeOOH
N Fe_3O_4 + GR*
P: $Fe^{II}Fe^{III}_5O_{12}H_9CO_3$
I
Fe(III)
Fe(II)
F
3
2.5
2
1.67
1.5
1
0.5
0
0
0.2
0.33
0.4
0.6
0.67
0.8
1
Mass balance diagram of iron compounds
$x_{Fe(III)} = \{n_{Fe(III)} / (n_{Fe(II)} + n_{Fe(III)})\}$

Microbially Influenced Corrosion and Marine Corrosion

A field study: **Steel sheet piles in harbours**

(With Laboratoire Central des Ponts et Chaussées, Dr A. Raharinaivo)

[20] J.-M. R. Génin, A. A. Olowe, N. .D. Benbouzid-Rollet, D. Prieur, M. Confente, and B. Résiak, *Hyp. Int*. **69** (1991) 875.

[21] J.-M. R. Génin, A. A. Olowe, B. Résiak, N. D. Benbouzid-Rollet, M. Confente, and D. Prieur, in **Marine Corrosion of Stainless Steels: Chlorination and Microbial Effects.** European Federation Corrosion Series n°10, (The Institute of Metals, London, 1993) p. 162.

The harbour: **Boulogne sur Mer** (late eighties)

Wharf, half a mile long, built on big piles supporting cranes, trains and many heavy materials.

Piles were 15 m high, made from 1 cm thick plain carbon steel sheets surrounding heavy stone blocks, gravel and sand. The external steel sheets displayed huge holes under the fouling crust, 10 cm thick, at a very specific level, that of the lowest tide (solstices), after only some years of service whereas they were planned for at least half a century.

The corrosion diagnosis was MIC and Mössbauer spectroscopy revealed that the rust, above the hole level, was essentially constituted of sulphated green rust and magnetite.

Some years later, the Coal and Steel European Community committed a contract to study the disorders about similar phenomena observed in other harbours. Involved companies were British Steel, Usinor (Unimétal), Hoescht, Arbed, i.e. makers of thick sheets. The disorders were found in harbours of the Atlantic Ocean, English Channel, North Sea and Baltic Sea. Curiously, there was no major problem in the Mediterranean Sea.

Anoxic conditions for long periods → MIC.

Strains of bacteria?

Level and specificity of pollution?

Eddy currents and redox potential?

No definite answer was then proposed, except that it was most probably MIC.

How do we explain today all these features?

Marine corrosion of steel

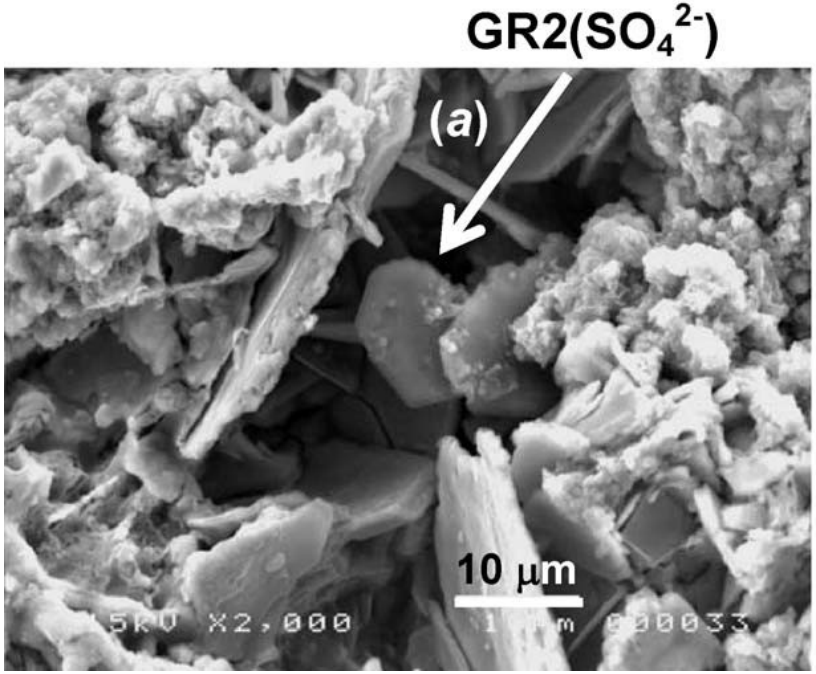

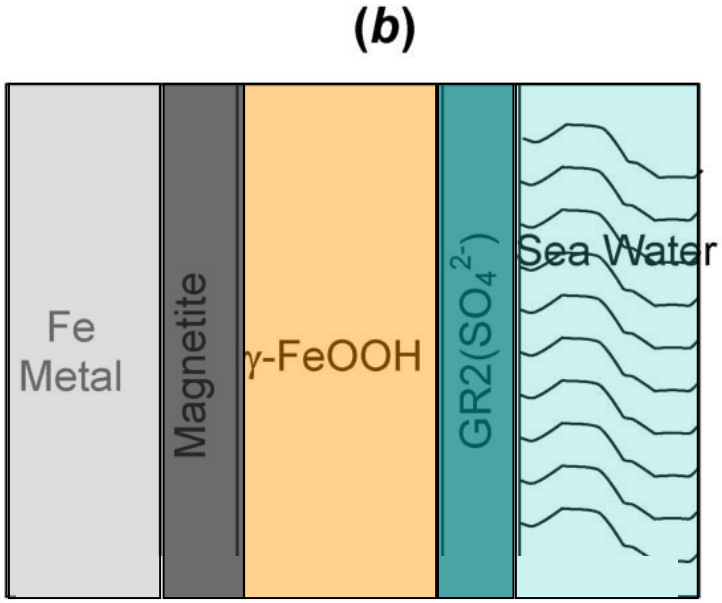

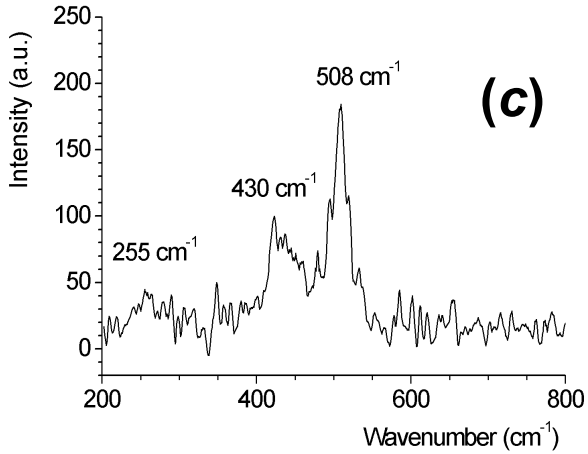

(a) SEM micrograph showing hexagonal shaped crystals of GR(SO_4^{2-}) upon corroded steel sheet left 25 years in seawater, (b) sequence of the rust layers: metal–magnetite–lepidocrocite–GR(SO_4^{2-}), (c) Raman spectrum of the outer part of the marine corroded layer.

Formation of the Fe(II)-Fe(III) hydroxysulphate green rust during marine corrosion of steel, Ph. REFAIT, J.B. MEMET, C. BON, R. SABOT and J.-M. R. GÉNIN *Corrosion Science* 2003, 45, 833-845

Asfaw Zegeye

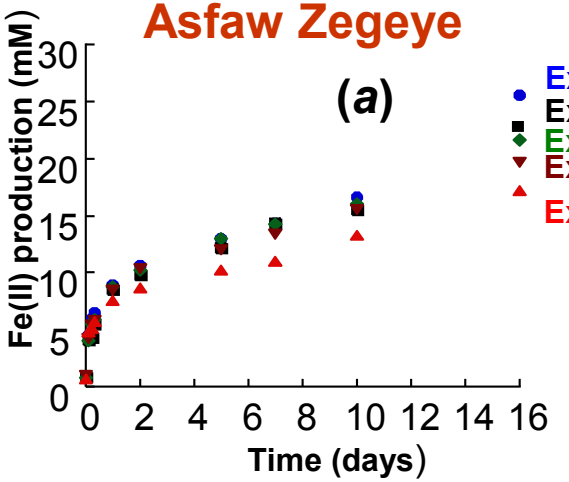

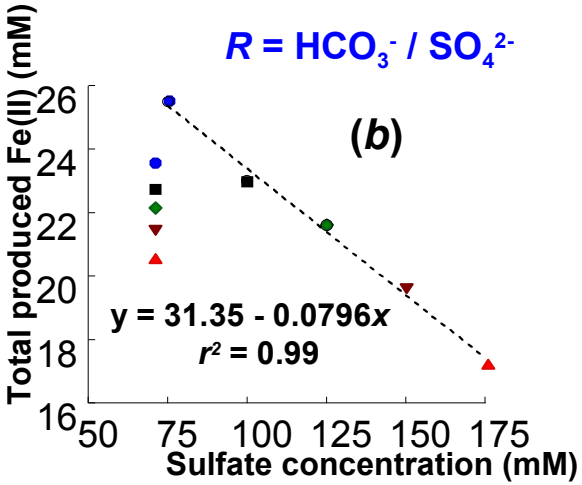

Formation of GR2(SO_4^{2-}) during the reduction of γ-FeOOH by a dissimilatory iron-respiring bacterium, *Shewanella putrefaciens*. Reduction was performed in a non-buffered medium without any organic compounds and with 25 mM of sulphate and with a range of lepidocrocite concentrations with H_2 as the electron donor under nongrowth conditions.

(a) Fe(II) production during bacterial reduction of lepidocrocite (80 mM) with formate (30 mM) in the presence of various concentrations of sulphate ions (from 75 to 175 mM). All experiments were realized at 31 ± 1°C with an initial pH of 7.6.
(b) Relationship between Fe(II) production and sulphate concentration.

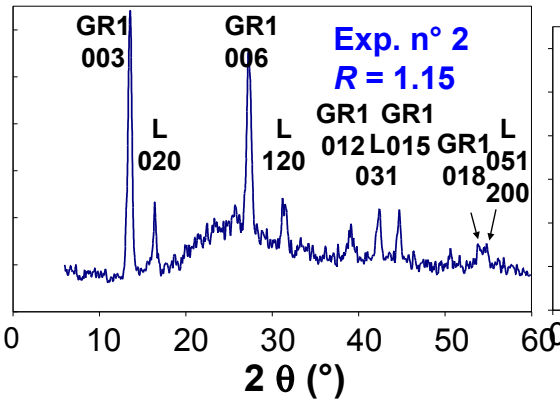

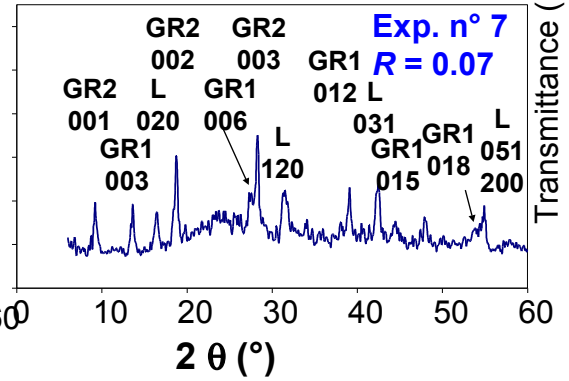

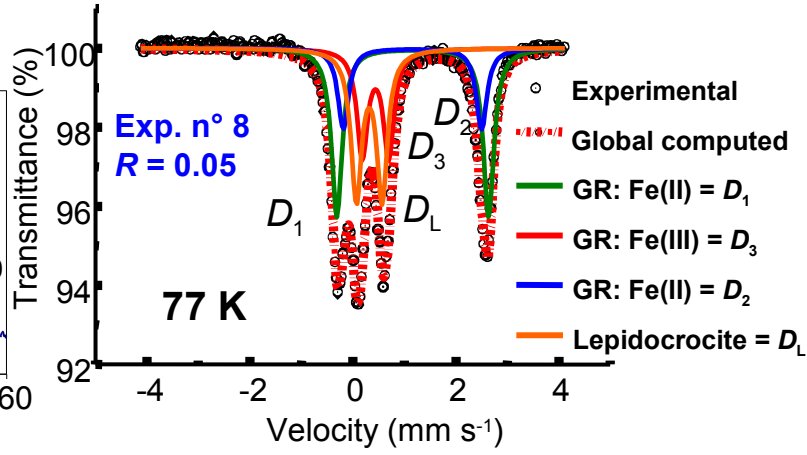

The resulting biogenic solids, after iron-respiring activity, were characterized by X-ray diffraction (XRD), transmission Mössbauer spectroscopy (TMS) and electron microscopy (SEM and TEM). The sulphate has been identified as the intercalated anion by diffuse reflectance infrared Fourier transform spectroscopy (DRIFTS). In addition, the structure of this sulphate anion was discussed. Our experimental study demonstrated that, under H_2 atmosphere, the biogenic solid was a GR2($SO4^{2-}$), as the sole iron(II-III) bearing mineral, whatever the initial lepidocrocite concentration. The crystals of the biotically formed GR2(SO_4^{2-}) are significantly larger than those observed for GR2(SO_4^{2-}) obtained through abiotic preparation, < 15 µm diameter as against 0.5-4 µm, respectively.

Asfaw Zegeye

$R = HCO_3^- / SO_4^{2-}$

(*a*) Exp. n° 2,
with 25 mM of sulfate and *R* = 1.15

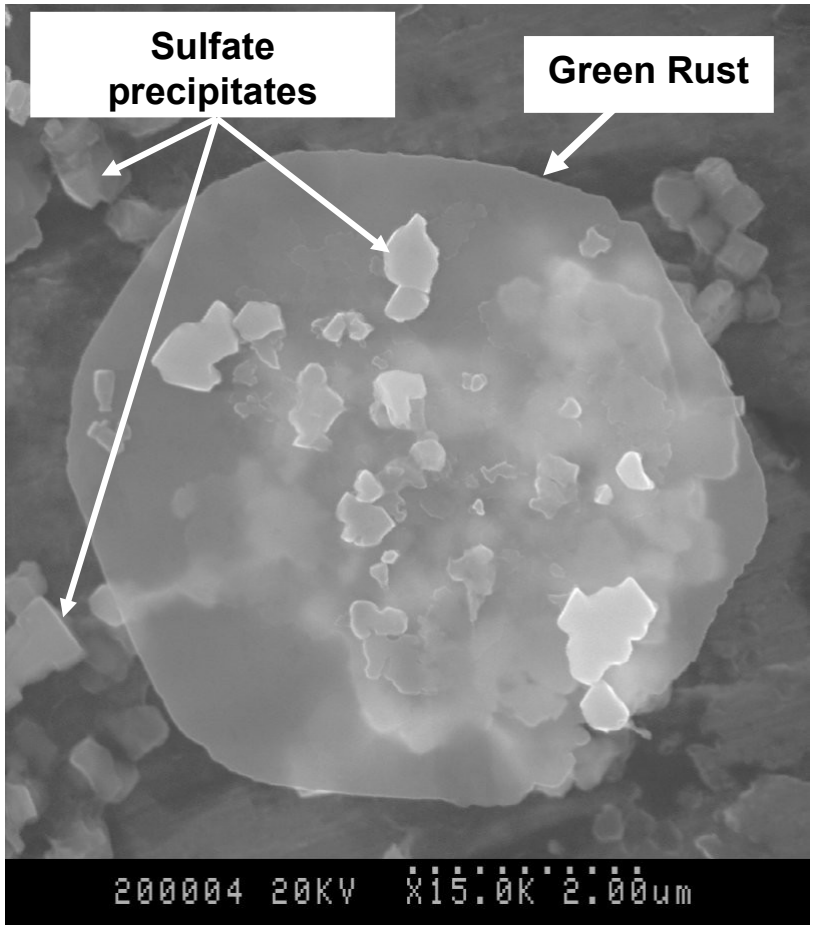

(b) Exp. n° 4,
with 75 mM of sulfate and *R* = 0.17

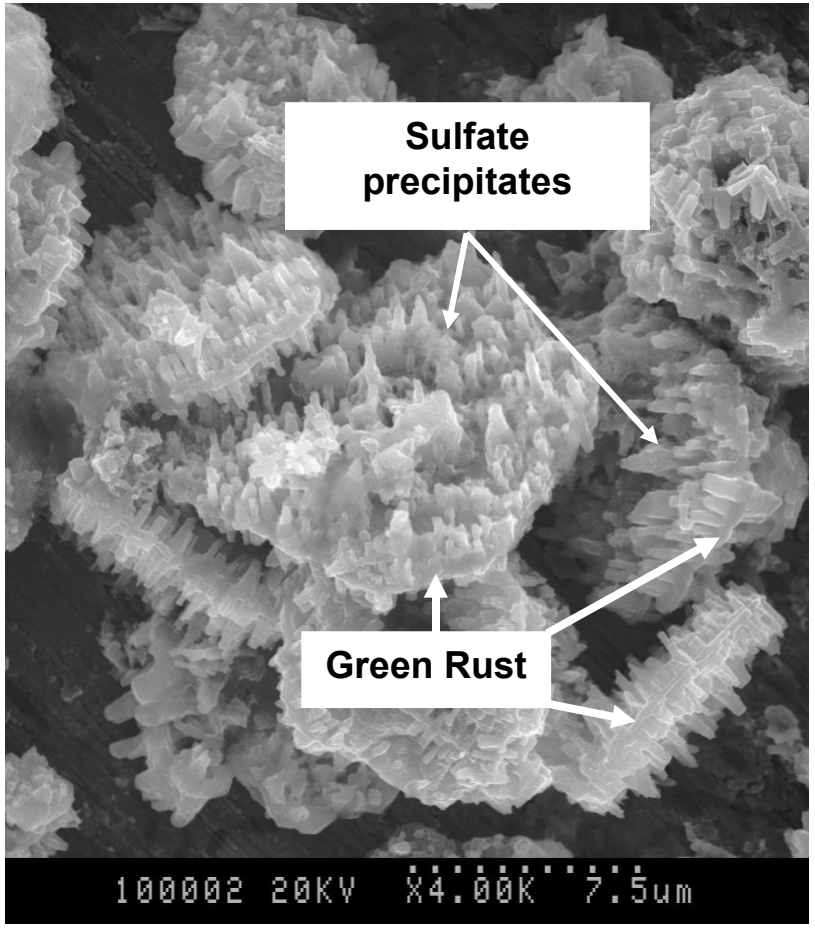

• Marine corrosion of steel

• The competition between GR1(Cl^-) & GR2(SO_4^{2-})

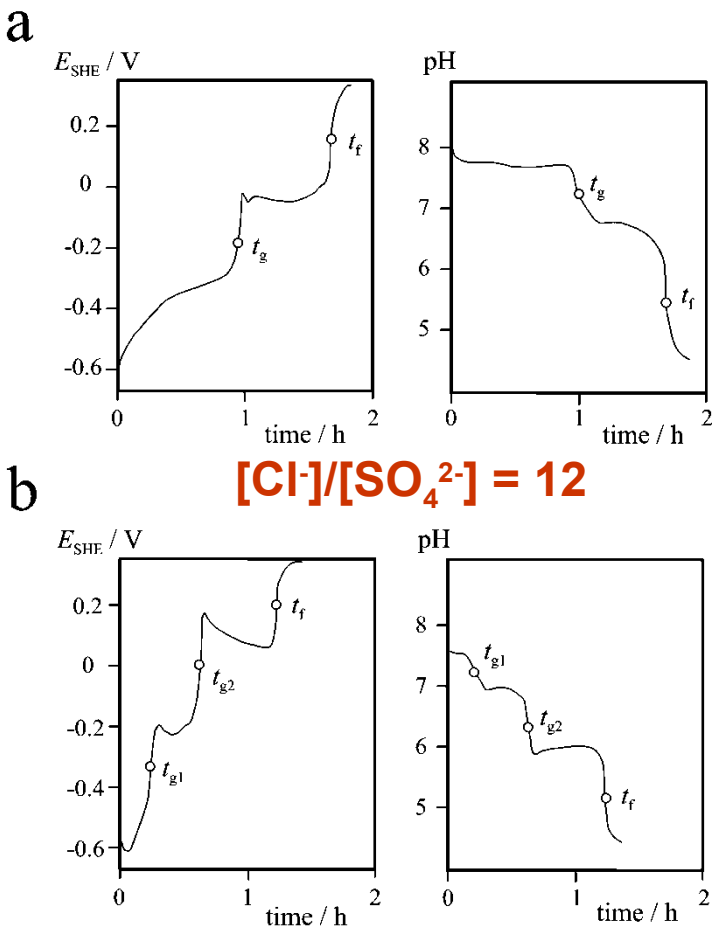

$[Fe^{2+}]/[OH^-] = 0.58$

$[Fe^{2+}]/[OH^-] = 1$

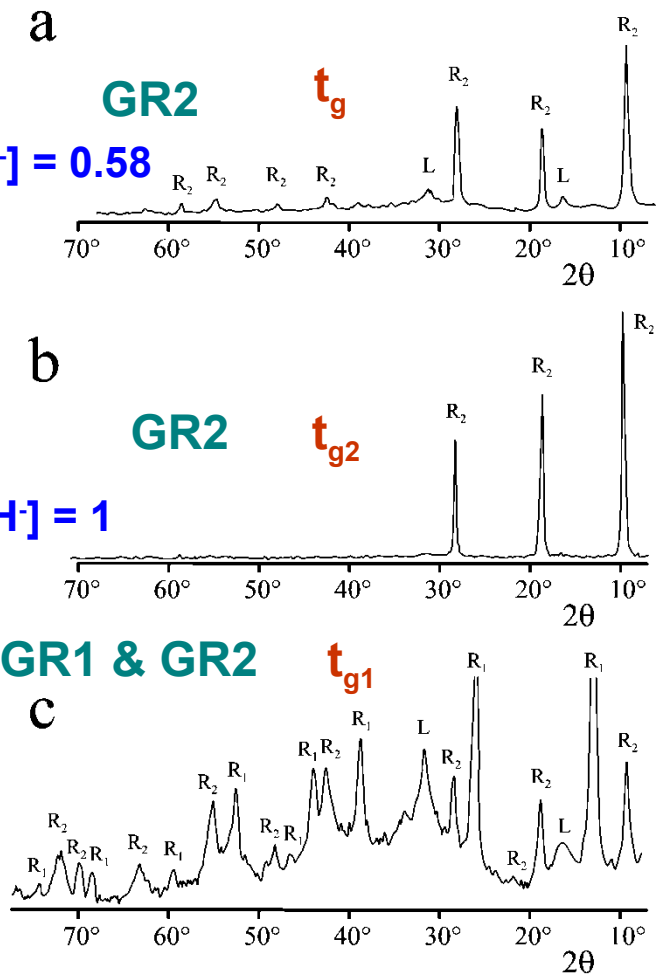

E_{SHE} (V vs SHE) and pH vs. time curves obtained during the oxidation of aqueous suspensions of Fe(II)-containing precipitates in the presence of Cl^- and SO_4^{2-} ions.
$[Cl^-]/[SO_4^{2-}] = 12$. (a) $[Fe^{2+}]/[OH^-] = 0.58$; (b) $[Fe^{2+}]/[OH^-] = 1$

Microbially influenced corrosion and Marine corrosion

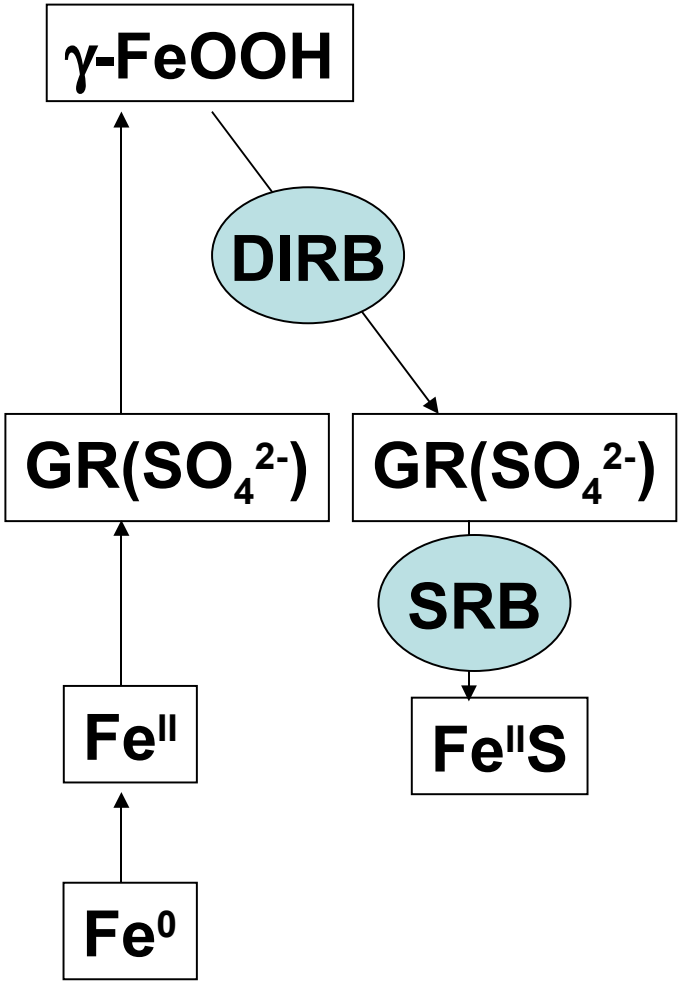

- **Ferric oxyhydroxides are reduced by dissimilatory iron-reducing bacteria,**
- **e.g. forming GR2(SO_4^{2-}) in sea water**
- **Then, GR2(SO_4^{2-}) is reduced into FeS by sulphate reducing bacteria**

- The morphology of **gley soils**, first described in 1905 by G. N. Vysostskii[1], remained a mystery up till recently when Mössbauer spectroscopy has been the determining tool to identify the iron containing compound that lies in **a horizon formed under waterlogged conditions in an anaerobic environment**, which encourages the reduction of iron compounds by microorganisms and often causes mottling of soil into a patchwork of greenish-blue-grey and rust colors. This finding is of utmost practical importance since there exists a correlation between the concentration of some pollutants and that of Fe^{II} ions that are dissolved in the water table. For instance, nitrates disappear where Fe^{II} appear in the anaerobic zone by following the water level in equilibrium with a mineral, which has been given the name of fougerite (IMA 2003-05). It occurs to be the **Fe^{II-III} oxyhydroxycarbonate** of formula $\mathbf{Fe^{II}_{6(1-x)}\ Fe^{III}_{6x}\ O_{12}\ H_{2(7-3x)}\ CO_3}$ where the domain of x is limited to [0.33-0.67].
- Originally studied for explaining the corrosion of iron-based materials, Fe^{II-III} hydroxysalts belong to the family of layered double hydroxides (LDH) and are constituted of **layers, $[Fe^{II}_{(1-x)}\ Fe^{III}_{x}\ (OH)_2\ ]^{x+}$**, and **interlayers, $[(x/n)A^{n-}\bullet(mx/n)H_2O]^{x-}$**. Here, we shall consider only the case where the anion is CO_3^{2-}.

- [1]G. N. Vysostskii, Gley, Pochvovedeniye, 4 (1905) 291-327.

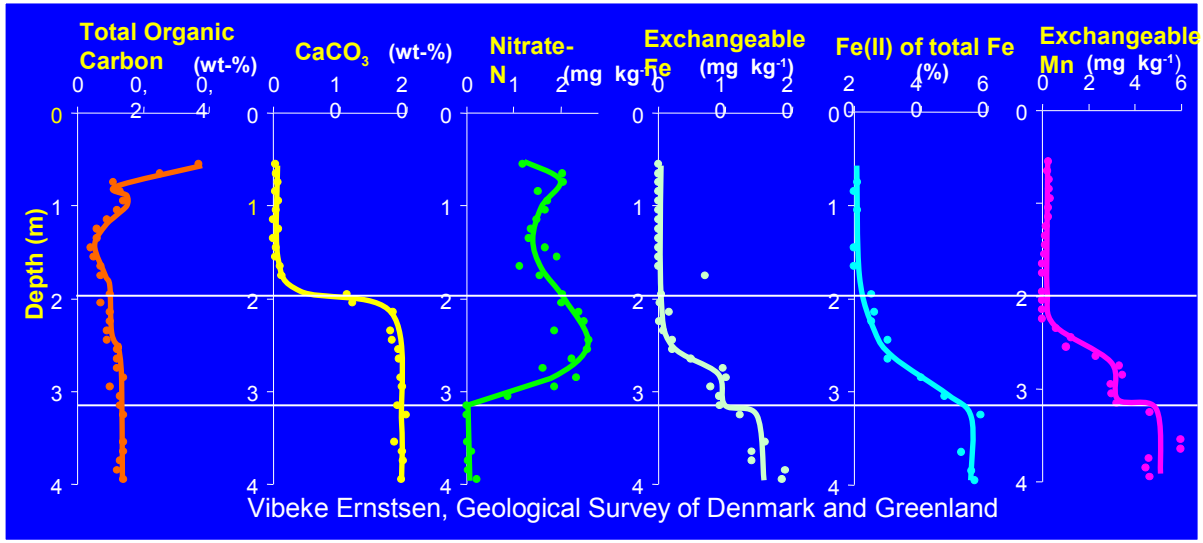

Depth profile analysis of a gleysol in Denmark through the redox zone between 2 and 3 meters deep. From left to right: Concentration of total organic carbon, calcium carbonate, nitrate, exchangeable iron, {[Fe^{II}] / [Fe_{total}]} and exchangeable Mn. Nitrates disappear when Fe^{II} appears.

Vibeke Ernstsen

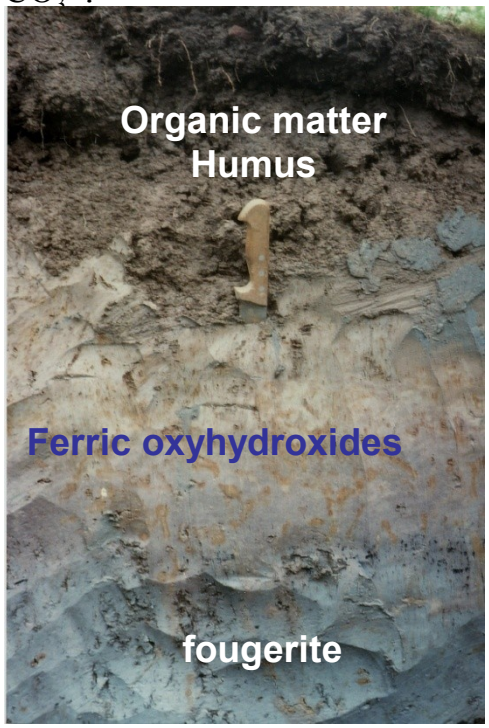

Hydromorphous gley soil profile

Valley of the Vraine river, 10 km north of Vittel (France)

Comparison between field experiments and laboratory assays

The similarity between the original spectrum obtained in 1996[1] (a) and that of the deprotonated oxyhydroxycarbonate[2] (b) is striking. More recently, field experiments were done in Fougères using **back-scattering miniaturized Mössbauer spectrometer MIMOS**[3] (c) to follow the value of ratio *x* with time and depth *in situ* within the gley soil.

(d) The fougerite mineral is able to reduce pollutants within the water table such as nitrates. Dissimilatory iron reducing bacteria regenerate the fougerite active mineral[4].

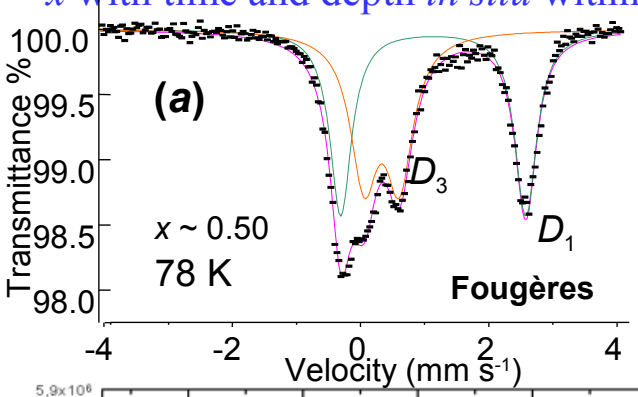

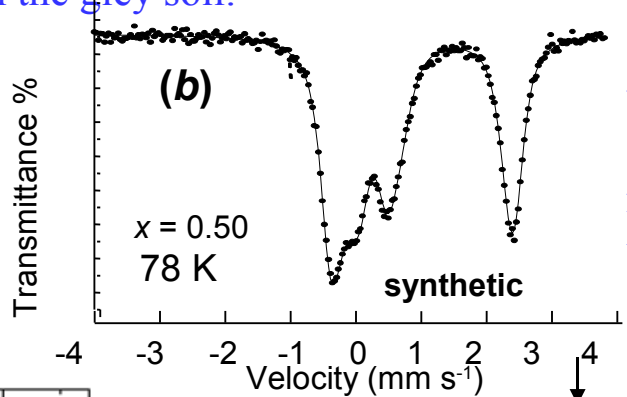

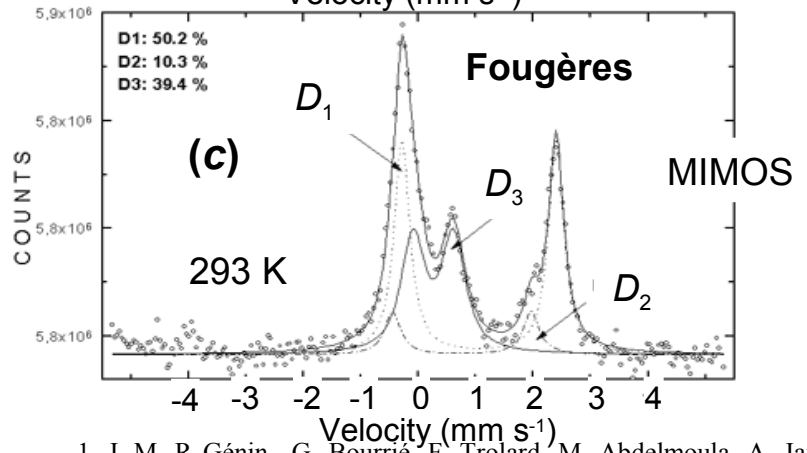

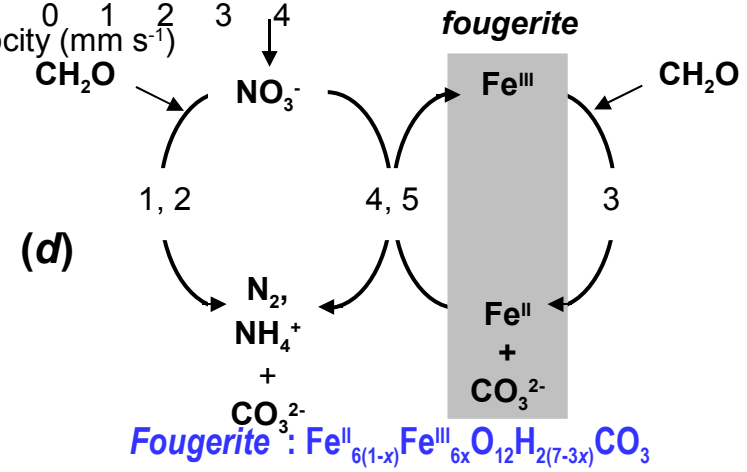

Fougerite : $Fe^{II}_{6(1-x)}Fe^{III}_{6x}O_{12}H_{2(7-3x)}CO_3$

1. J.-M. R Génin., G. Bourrié, F. Trolard, M. Abdelmoula, A. Jaffrezic, Ph. Refait, V. Maître, B. Humbert and A. Herbillon, Thermodynamic equilibria in aqueous suspensions of synthetic and natural Fe(II) - Fe(III) green rusts; occurences of the mineral in hydromorphic soils, *Environ. Sci. Technol.* 32 (1998) 1058-1068.

2. J.-M. R. Génin, R. Aïssa, A. Géhin, M. Abdelmoula, O. Benali, V. Ernstsen, G. Ona-Nguema,C. Upadhyay and C. Ruby, Fougerite and FeII–III hydroxycarbonate green rust; ordering, deprotonation and/or cation substitution; structure of hydrotalcite-like compounds and mythic ferrosic hydroxide Fe(OH)(2+x), *Solid State Sci.,* 7 (2005) 545-572.

3. D. Rodionov, G. Klingelhöfer, B. Bernhardt, C. Schröder, M. Blumers, S. Kane, F. Trolard, G. Bourrié, and . J.-M. R. Génin, Automated Mössbauer spectroscopy in the field and monitoring of fougerite, *Hyperfine Interactions*, 167 (2006) 869-873.

4. C. Ruby, C. Upadhyay, A. Géhin, G. Ona-Nguema and J.-M. R. Génin, *In situ* redox flexibility of FeII-III oxyhydroxycarbonate green rust and fougerite, *Environ. Sci. Technol.*, 40 (2006) 4696-4702.

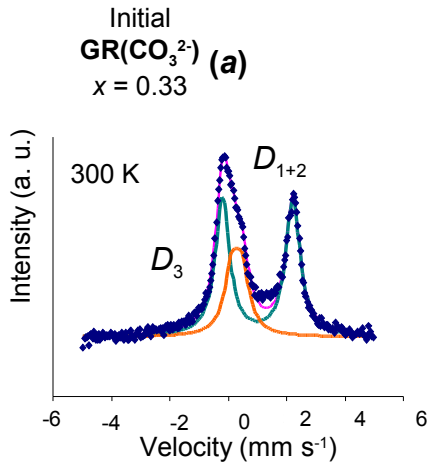

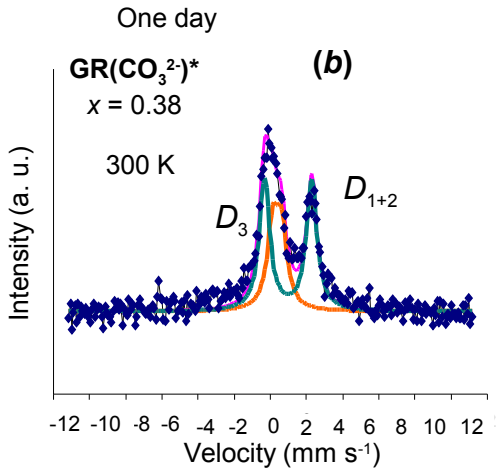

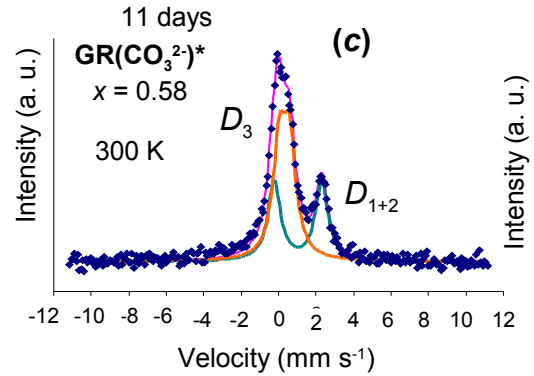

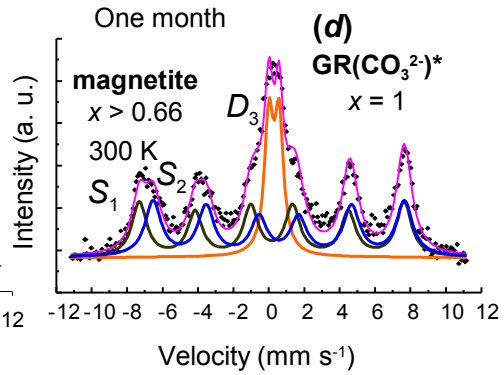

Nitrate reduction and *In situ* oxidation of $GR(CO_3^{2-})^*$

Typical time of half reaction is one week

$$Fe^{II}_{6[1-(x+dx)]}\,Fe^{III}_{6(x+dx)}\,O_{12}\,H_{2[7-3(x+dx)]}\,CO_3 + (6\times dx)\,H^+ + (6\times dx)\,e^- \rightarrow Fe^{II}_{6(1-x)}\,Fe^{III}_{6x}\,O_{12}\,H_{2(7-3x)}\,CO_3$$

or

$$GR^*(x+dx) + dx\,H^+ + dx\,e^- \rightarrow GR^*(x)$$

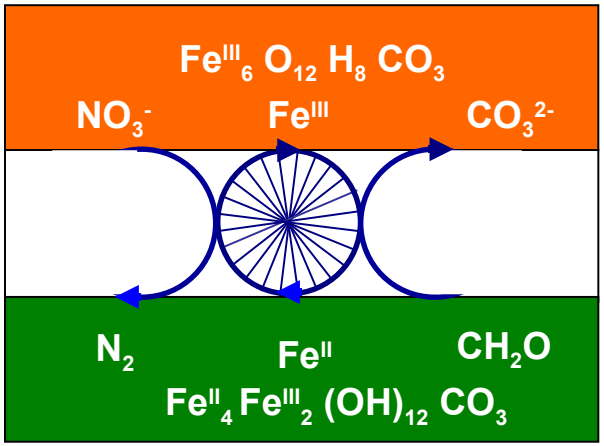

x Fig T	$GR(CO_3^{2-})$ at 0.33 (a) 300 K initial			$GR(CO_3^{2-})^*$ at 0.38 (b) 300 K, one day			$GR(CO_3^{2-})^*$ at 0.58 (c) 300 K,11 days			$GR(CO_3^{2-})^*$ 1.00 and magnetite (d) 300 K, one month			
	δ mm s^{-1}	Δ mm s^{-1}	*RA* (%)	δ mm s^{-1}	Δ mm s^{-1}	*RA* (%)	δ mm s^{-1}	Δ mm s^{-1}	*RA* (%)	δ mm s^{-1}	Δ mm s^{-1}	*H* kOe	*RA* (%)
D_{1+2}	1.12	2.4	67	0.98	2.6	62	1.03	2.53	42				
D_3	0.41	0.35	33	0.37	0.49	38	0.31	0.55	58	0.4	0.57		20
S_1										0.27		463	39
S_2										0.67		440	41

δ, isomer shift in mm s^{-1} (metallic iron as reference at room temperature); Δ quadrupole splitting in mm s^{-1}; *RA* in %: relative abundance. Half widths at half maximum are 0.3, 0.35, 0.4 and 0.6 mm s^{-1}.

Fougerite is the active mineral that is mixed with clay minerals and responsible for the natural reduction of nitrates in gley soils within the water table.

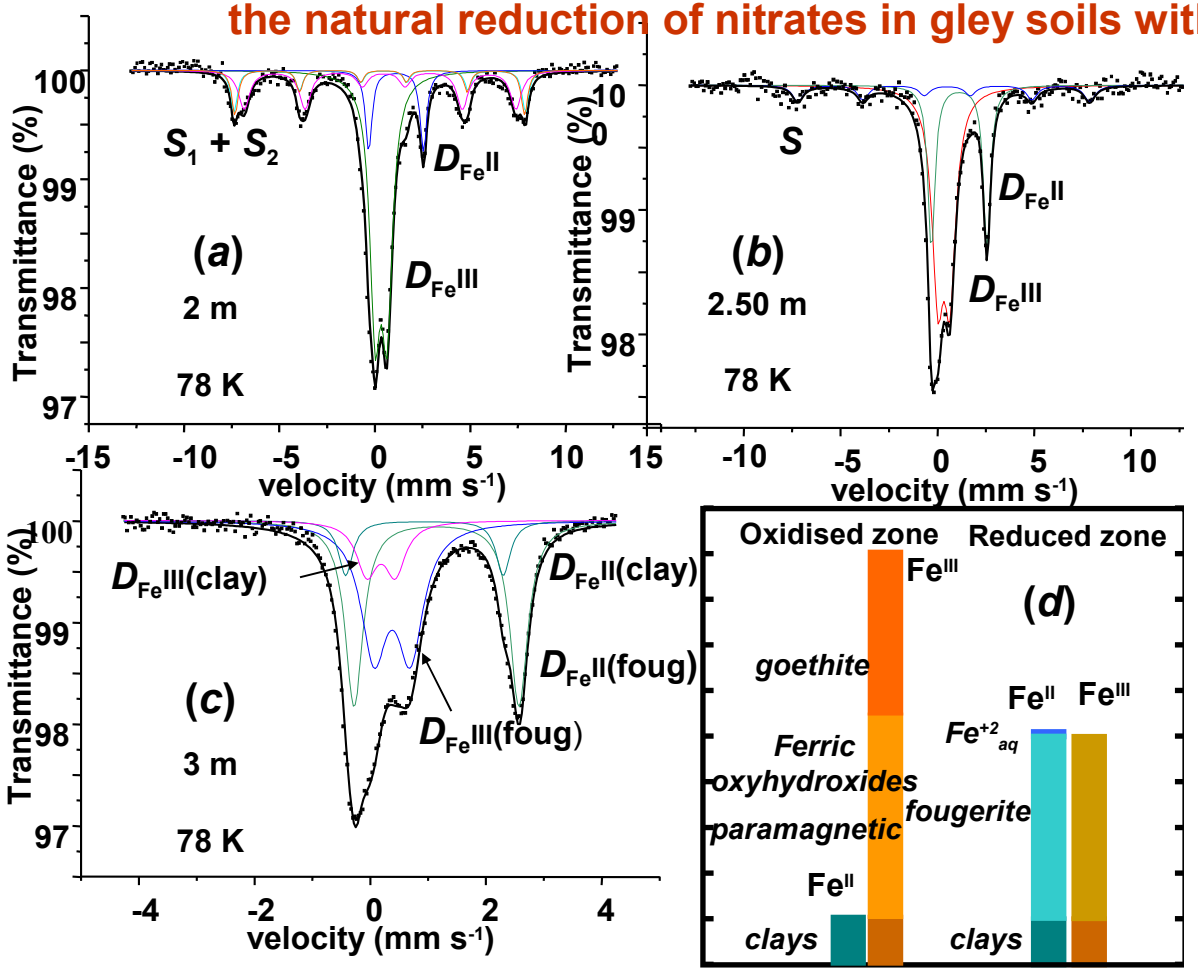

	δ (mm s⁻¹)	Δ (mm s⁻¹)	H (kOe)	Γ (mm s⁻¹)	RA (%)
Depth 2 m					
D_{Fe}III (para +clay)	0.39	0.65		0.67	55
(para +clay)					
D_{Fe}II (clay)	1.17	2.85		0.41	11.7
S_1 (goethite)	0.37	−0.21	474	0.41	10.6
S_2 (goethite)	0.38	−0.19	442	0.70	22.5
S_1 +S_2 (goethite)					33
Depth 2.50 m					
D_{Fe}III (para+clay+foug)	0.39	0.62		0.72	57.7
D_{Fe}II (clay+ foug)	1.18	2.86		0.44	30.4
S (goethite)	0.43	−0.19	468	0.68	11.8
Depth 3 m					
D_{Fe}II (foug)	1.17	2.84		0.37	39
D_{Fe}III (foug)	0.39	0.63		0.55	40.5
D_{Fe}II (clay)	0.96	2.71		0.30	9
D_{Fe}III (clay)	0.20	0.48		0.42	11.5

Hyperfine parameters of Mössbauer spectra measured at 78 K of samples extracted in Denmark at different depths of 2 m, 2.50 m, 3 m out of hydric soils from (a) an oxidised zone to (c) a reduced zone. A mixture of fougerite, ferric oxyhydroxides and clay minerals is observed. *H*: hyperfine field (kOe); *δ*: isomer shift (mm s⁻¹) with respect to *α* Fe at room temperature; *Δ* or *ε*: quadrupole splitting or shift (mm s⁻¹); *Γ* : half-width at half maximum (mm s⁻¹); *RA*: relative abundance (%).

J.-M. R. Génin, R. Aïssa, A. Géhin, M. Abdelmoula, O. Benali, V. Ernstsen, G. Ona-Nguema,C. Upadhyay and C. Ruby, Fougerite and Fe^{II-III} hydroxycarbonate green rust; ordering, deprotonation and/or cation substitution; structure of hydrotalcite-like compounds and mythic ferrosic hydroxide $Fe(OH)_{(2+x)}$, *Solid State Sci.*, 7 (2005) 545-572.

COMPTES RENDUS GEOSCIENCE
Académie des sciences – Paris
Rouilles vertes / *Green rusts* •
Tome 338 • No 6–7 • 393–498 •
GEOSCIENCE
Tome 338 Juin 2006
fascicule 6–7 ISSN 1631-0713
Numéro thématique / *Thematic issue*
Les rouilles vertes et la fougérite dans le cycle biogéochimique du fer
Green rusts and fougerite in the biogeochemical cycle of iron
Rédacteurs invités / *Guest Editors:*
Adrien J. Herbillon,
Jean-Marie R. Génin

Remerciements / *Acknowledgments*

Hoping to have forgotten nobody

1980

D. Rézel
Ph. Bauer
A. Béral
A. Raharinaivo
A. Olowe
J. Guézennec
M. Pourbaix
D. Prieur
N. Benbouzid-Rollet
B. Resiak
Ph. Refait
B. Pauron

1990

M. Abdelmoula
Y. Marie
H. Drissi
A. Herbillon
G. Bourrié
F. Trolard
A. Jaffrezic
B. Humbert
C. Bon
J. Bessière
A. Charton
L. Simon
C. Ruby
M. François
M. Lelaurain
S. Loyaux-Lawniczak
A. Géhin
F. Jorand
G. Ona Nguema

2000

O. Benali
L. Dhouibi
E. Triki
L. Legrand
A. Chaussé
F. Bocher
G. Klingelhöfer
F. Féder
J.P. Jolivet
R. Aïssa
C. Carteret
A. Zegeye
V. Ernstsen
C. Upadhyay
V. Khare
B. Rusch
P. Bonville
A. Renard

In red: thesis about
Green rusts or fougerite


No.1
Viele Danke